

AN ENERGY STABLE WELL-BALANCED SCHEME FOR THE BAROTROPIC EULER SYSTEM WITH GRAVITY UNDER THE ANELASTIC SCALING

K. R. ARUN AND MAINAK KAR

ABSTRACT. We design and analyse an energy stable, structure preserving, well-balanced and asymptotic preserving (AP) scheme for the barotropic Euler system with gravity in the anelastic limit. The key to energy stability is the introduction of appropriate velocity shifts in the convective fluxes of mass and momenta. The semi-implicit in time and finite volume in space fully-discrete scheme supports the positivity of density and yields the consistency with the weak solutions of the Euler system upon mesh refinement. The numerical scheme admits the discrete hydrostatic states as solutions and the stability of numerical solutions in terms of the relative energy leads to well-balancing. The AP property of the scheme, i.e. the boundedness of the mesh parameters with respect to the Mach/Froude numbers and the scheme's asymptotic consistency with the anelastic Euler system is rigorously shown on the basis of a priori energy estimates. The numerical scheme is resolved in two steps: by solving a non-linear elliptic problem for the density and a subsequent explicit computation of the velocity. Results from several benchmark case studies are presented to corroborate the proposed claims.

1. INTRODUCTION

The Euler equations of inviscid compressible fluid dynamics are invariably one of the most commonly used set of equations to model non-hydrostatic atmospheric processes. These equations have a complex wave-structure consisting of advection waves, gravity waves and acoustic waves or sound waves. Though the sound waves are not of much relevance in atmospheric flow calculations, they introduce a lot of difficulties in the numerical integration of flow equations due to their large characteristic speeds. Developing efficient methods for handling fast acoustic waves is still an active area of research. In the realm of atmospheric flow computations, the so-called sound-proof models constitute a good alternative to using the full set of compressible Euler equations. The sound-proof models are usually derived via approximating the Euler equations by eliminating fast acoustic waves, at the same time retaining meteorologically relevant advection and internal gravity waves. For the Euler equations, the two characteristic parameters which quantify the effects due to compressibility and gravitational stratification are, respectively, the Mach and Froude numbers. It is relevant to derive sound-proof models for atmospheric and astrophysical flows by considering the scenario when the Mach and Froude numbers diminish to zero at the same rate. The resulting regime, wherein the flow becomes incompressible and stratified simultaneously at the same pace, can be represented by a sound-proof equation system called the anelastic equations [39]. In the meteorological literature, different types of anelastic models which vary in the way they account for density or temperature stratifications and internal gravity waves can be found [36]. The forerunners

Date: May 2, 2024.

2020 Mathematics Subject Classification. Primary 35L50, 35L60, 35L65, 35L67; Secondary 65M08, 65M12.

Key words and phrases. Euler equations with gravity, Well-balanced, Anelastic limit, Asymptotic preserving, Finite volume method, MAC grid, Energy stability.

K. R. A. gratefully acknowledges the Core Research Grant - CRG/2021/004078 from the Science and Engineering Research Board, Department of Science & Technology, Government of India.

among them are the anelastic model of Ogura and Philips [40], the anelastic model of Bannon [4] and the pseudo-incompressible model of Durran [17].

From a mathematical point of view, the Ogura and Philips anelastic approximation of the Euler system via the vanishing limit of the Mach and Froude numbers corresponds to performing a singular limit of the governing equations whereby the Euler system changes its nature from hyperbolic to mixed hyperbolic-elliptic; see, e.g. [9, 20, 24, 38] for rigorous and detailed accounts on various sound-proof limits. Consequently, a feasible platform to build a numerical Euler solver for multiscale atmospheric flow applications turns out to be the so-called ‘Asymptotic Preserving’ (AP) methodology [34]. The AP framework is a generic, yet powerful, tool for approximating singularly perturbed problems. When applied to a stratified atmospheric flow simulation, an AP scheme can automatically emulate the flow features in the singular (anelastic), non-singular (compressible) as well as the intermediate (weakly compressible) regions where the regime changes can occur. The working principle behind the AP methodology is as follows. Suppose P^ε denote a singularly perturbed problem, such as the scaled compressible Euler equations containing small Mach and Froude numbers denoted by an infinitesimal ε . In the singular limit $\varepsilon \rightarrow 0$, suppose the problem P^ε converges to a well-posed limit problem P^0 ; e.g. the anelastic model. An AP scheme respects the above convergence at the discrete level in the following sense.

- (i) Let h denote the space-time discretisation parameter. For each $\varepsilon > 0$, let P_h^ε denote a consistent discretisation of the problem P^ε , i.e. $P_h^\varepsilon \rightarrow P^\varepsilon$ as $h \rightarrow 0$.
- (ii) For a fixed discretisation h , the scheme P_h^ε goes to P_h^0 as $\varepsilon \rightarrow 0$, where P_h^0 denotes a consistent scheme for the limit problem P^0 , i.e. $P_h^0 \rightarrow P^0$ as $h \rightarrow 0$.
- (iii) The stability constraints on the discretisation parameter h remain independent of ε .

A rather common practice to develop AP schemes for time-dependent partial differential equations, such as the Euler equations, is to employ an implicit-explicit (IMEX) or semi-implicit time discretisation [7]. Compared to their fully-implicit counterparts, a semi-implicit formalism has the advantage that it minimises the need to invert large and dense matrices. However, the challenge is to maintain the optimal level of implicitness so as to overcome the stiffness imposed by the time-step restrictions and achieve computational efficiency at the same time.

Models of gravity driven flows, such as the Euler equations with gravitational source terms, often describe a phenomenon where the force due to the gravity is balanced by the internal force. This balance of forces leads to an interesting stationary solution, known as the hydrostatic steady state, which corresponds to a static fluid with the corresponding pressure gradient exactly in balance with the weight of the fluid. Most of the atmospheric flow problems of practical interest can be described as small perturbations of the hydrostatic steady state [18]. Furthermore, the derivation of Ogura and Philipps anelastic approximation of the Euler equations by a scale analysis [18, 40] or a zero Mach number asymptotic analysis [35] reveals that the ambient flow or the leading order solution is in hydrostatic balance. Consequently, it is much desirable that numerical schemes for the Euler equations with gravity, particularly in the anelastic regime, be capable of preserving the steady states at a discrete level while accurately emulating the flow features evolving from its perturbations. Unfortunately, classical numerical schemes often fail to preserve the steady states for a large time within an acceptable range of accuracy. A cure to this ailment is achieved by introducing the so-called ‘well-balanced’ schemes. A well-balanced scheme exactly satisfy the discrete counterparts of the steady states of the corresponding continuum equations. The well-balancing methodology has since been adopted and developed for formulating robust numerical schemes for several hydrodynamic models with source terms in the context of explicit time-stepping schemes; see, e.g. [3, 25, 31, 42] for a few references. However, establishing the well-balancing property of

IMEX or semi-implicit time discretisation schemes is a challenging task. Often, proving the balance for implicit time discretisations involve solving nonlinear algebraic equations for the pressure or density. The literature in this direction is rather sparse; see, e.g. [5, 6, 41] and the references therein.

The aim of the present work is to design and analyse a semi-implicit, AP, well-balanced, energy stable and structure preserving finite volume scheme for the barotropic Euler system with gravity in the anelastic limit. An optimal semi-implicit time discretisation is adopted to overcome the stiffness posed by the pressure gradient and gravitational terms. Since the solutions of hyperbolic systems are known to develop discontinuities in finite time, additional stability requirements are to be imposed to single out physically valid weak solutions. Numerical schemes that respect important physical stability properties of the corresponding continuum equations, such as preserving the positivity of mass density, respecting the second law of thermodynamics (entropy stability) and so on, are sometimes referred to as invariant domain preserving or structure preserving methods. Consequent to the semi-implicit treatment of the fluxes, the present scheme achieves the energy stability a priori under a CFL-like time-step restriction. An application of the tools from topological degree theory in finite dimensions helps in proving the existence of a numerical solution and the positivity of density. The scheme is weakly consistent with the continuous equations as the mesh parameters go to zero à la Lax-Wendroff. We employ the so-called relative energy, defined with respect to a hydrostatic equilibrium state, as a measure to establish the energy stability. The relative energy is a powerful tool that can be adopted to obtain uniform estimates on the solutions and to perform rigorous asymptotic limits of the continuous equations [24] as well as their numerical approximations [1, 22, 33]. Interestingly, in the present work, we show that using relative energy not only facilitate the entropy stability but also gives another crucial benefit, namely the provability of both the well-balancing and AP properties. Our careful design to achieve these salient features involves two key ingredients. The first is introducing a shift in the velocity in the discrete convective fluxes of mass and momenta as in [15, 16] to get the dissipation of mechanical energy. The second is a novel treatment of the discrete density on the interfaces, while discretising the mass flux and the stiff gravitational source term. This particular interface discretisation, referred to as the ‘ γ -mean’ with γ being the adiabatic constant, helps in emulating the entropy balance at the discrete level, and subsequently leads to the well-balancing and AP properties. The stability of solutions with respect to the relative energy ensures that any initial steady state remains preserved during the subsequent updates. In other words, the discrete energy stability renders the scheme well-balanced. The stability also guarantees that numerical solutions generated from initial conditions that are given in terms of perturbations of the steady state remain numerically stable, i.e. no spurious solutions are generated. The discrete relative energy stability further leads to a priori estimates on the solution which enables us to perform a rigorous asymptotic convergence analyses with respect to the singular parameters, i.e. the Mach and Froude numbers. Consequently, we establish the AP property of the scheme, where we rigorously prove that the proposed scheme for the compressible Euler system with gravity converges to a semi-implicit scheme for the anelastic Euler equations as the Mach and Froude numbers vanish. We wish to emphasise that this is the first time a finite volume scheme has been developed for the barotropic Euler system with gravitational source term, which is at the same time provably energy stable, well-balanced, AP and positivity preserving, to the best of our knowledge.

The rest of this paper is organised as follows. In Section 2 we review a few results regarding the scaled barotropic Euler system with gravity and its anelastic limit. Section 3 provides an outline of the domain discretisation along with the discrete differential operators in a finite volume framework. The final scheme and the description of the discrete hydrostatic steady state is described in Section 4. Section 5 is devoted to prove the energy stability and the well-balancing property of the proposed

scheme. In Sections 6 and 7 we give rigorous proofs of the consistency of the approximate solutions with respect to the weak solutions and the anelastic limit model respectively. Finally, in Section 8, we substantiate our claims regarding the salient properties of the scheme with several numerical case studies.

2. COMPRESSIBLE EULER SYSTEM WITH GRAVITY AND THE ANELASTIC LIMIT

We start with the following non-dimensional barotropic compressible Euler system with gravity, parametrised by the Mach and the Froude numbers, and posed for $(t, \mathbf{x}) \in Q_T := (0, T) \times \Omega$:

$$(2.1) \quad \partial_t \rho^\varepsilon + \operatorname{div}(\rho^\varepsilon \mathbf{u}^\varepsilon) = 0,$$

$$(2.2) \quad \partial_t(\rho^\varepsilon \mathbf{u}^\varepsilon) + \mathbf{div}(\rho^\varepsilon \mathbf{u}^\varepsilon \otimes \mathbf{u}^\varepsilon) + \frac{1}{\varepsilon^2} \nabla p^\varepsilon = -\frac{1}{\varepsilon^2} \rho^\varepsilon \nabla \phi.$$

Here, $T > 0$ and $\Omega \subset \mathbb{R}^d$, $d = 1, 2, 3$, is a bounded open connected subset and the dependent variables $\rho^\varepsilon = \rho^\varepsilon(t, \mathbf{x}) > 0$ and $\mathbf{u}^\varepsilon = \mathbf{u}^\varepsilon(t, \mathbf{x}) \in \mathbb{R}^d$ denote the fluid density and the fluid velocity, respectively. The pressure $p^\varepsilon = \wp(\rho^\varepsilon)$ is assumed to follow a barotropic equation of state $\wp(\rho) := \rho^\gamma$, with $\gamma > 1$ being the ratio of specific heats. The gravitational potential $\phi = \phi(\mathbf{x})$ is assumed to be a known, continuous function. The system (2.1)-(2.2) is supplied with the following initial and boundary conditions:

$$(2.3) \quad \rho^\varepsilon|_{t=0} = \rho_0^\varepsilon, \quad \mathbf{u}^\varepsilon|_{t=0} = \mathbf{u}_0^\varepsilon, \quad \mathbf{u}^\varepsilon \cdot \boldsymbol{\nu}|_{\partial\Omega} = \mathbf{0},$$

where $\boldsymbol{\nu}$ denotes the unit outward normal to the boundary $\partial\Omega$. Throughout this work, we assume that the system (2.1)-(2.2) is under the anelastic scaling so that the pressure gradient and the gravitational force term are of equal magnitude in the momentum equation (2.2). In other words, the Mach and the Froude numbers are scaled by the same power of the infinitesimal $\varepsilon \in (0, 1]$. Classical solutions to the initial boundary value problem (2.1)-(2.3) are known to develop discontinuities in finite time, which necessitates the definition of weak solutions. A weak solution of the system (2.1)-(2.2) in the conservative variables ρ^ε and $\mathbf{m}^\varepsilon = \rho^\varepsilon \mathbf{u}^\varepsilon$ is defined as follows.

Definition 2.1. The pair $(\rho^\varepsilon, \mathbf{m}^\varepsilon)$ is a weak solution of (2.1)-(2.2) if

(i) $\rho^\varepsilon > 0$ a.e. in $[0, T) \times \Omega$, and the identity

$$(2.4) \quad \int_0^T \int_\Omega (\rho^\varepsilon \partial_t \varphi + \mathbf{m}^\varepsilon \cdot \nabla \varphi) \, d\mathbf{x} dt = - \int_\Omega \rho_0^\varepsilon \phi(0, \cdot) \, d\mathbf{x}$$

holds for all $\varphi \in C_c^\infty([0, T) \times \bar{\Omega})$.

(ii) $\mathbf{m}^\varepsilon = \mathbf{0}$ whenever $\rho^\varepsilon = 0$, and the identity

$$(2.5) \quad \int_0^T \int_\Omega \left(\mathbf{m}^\varepsilon \cdot \partial_t \boldsymbol{\varphi} + \left(\frac{\mathbf{m}^\varepsilon \otimes \mathbf{m}^\varepsilon}{\rho^\varepsilon} \right) : \nabla \boldsymbol{\varphi} + \frac{1}{\varepsilon^2} p^\varepsilon \operatorname{div} \boldsymbol{\varphi} \right) \, d\mathbf{x} dt = - \int_\Omega \mathbf{m}_0^\varepsilon \cdot \boldsymbol{\varphi}(0, \cdot) \, d\mathbf{x} \\ + \frac{1}{\varepsilon^2} \int_0^T \int_\Omega \rho^\varepsilon \nabla \phi \cdot \boldsymbol{\varphi} \, d\mathbf{x} dt$$

holds for all $\boldsymbol{\varphi} \in C_c^\infty([0, T) \times \bar{\Omega})^d$.

The well-posedness of the Euler system (2.1)-(2.2) in the class of weak solutions as defined above is not well understood for general initial data; see [9, 10, 21] for more discussions. Throughout the present work, however, we assume the existence of a weak solution of (2.1)-(2.2) in order to carry out the numerical analysis.

2.1. Hydrostatic Steady States. In the numerical modelling of the Euler system with gravity, the hydrostatic steady state wherein the velocities vanish and the pressure gradient exactly balances the gravitational source term plays a vital role. For the scaled Euler system (2.1)-(2.2), the hydrostatic steady state is given by $\rho^\varepsilon = \tilde{\rho}$, $\mathbf{u}^\varepsilon = \mathbf{0}$, where the steady state density $\tilde{\rho}$ is independent of ε and can be obtained from the equilibrium condition

$$(2.6) \quad \nabla \tilde{p} = -\tilde{\rho} \nabla \phi.$$

Here, $\tilde{p} = \wp(\tilde{\rho})$ denotes the hydrostatic pressure. We can integrate (2.6) to readily yield

$$(2.7) \quad h'_\gamma(\tilde{\rho}) + \phi = C(m_0),$$

where the so-called Helmholtz function $h_\gamma: \mathbb{R}^+ \rightarrow \mathbb{R}$ is defined by

$$(2.8) \quad h_\gamma(\rho) := \frac{\rho^\gamma}{\gamma - 1}, \quad \rho \in \mathbb{R}^+,$$

and $C(m_0)$ is a constant of integration which can be determined by the total mass $m_0 = \int_\Omega \tilde{\rho}(\mathbf{x}) d\mathbf{x}$ at equilibrium. Note that h_γ is a convex function and it satisfies the following relation for all $\rho > 0$:

$$(2.9) \quad \rho h'_\gamma(\rho) - h_\gamma(\rho) = \wp(\rho).$$

Remark 2.2. For convenience, we assume that $\gamma > 1$ throughout the present work. The case $\gamma = 1$ can be handled in a similar fashion.

2.2. Apriori Energy Estimates. We can derive the following apriori estimates for classical solutions of the Euler system.

Proposition 2.3. *The following identities are satisfied by classical solutions of (2.1)-(2.2).*

(i) *A renormalisation identity:*

$$(2.10) \quad \partial_t h_\gamma(\rho^\varepsilon) + \operatorname{div}(h_\gamma(\rho^\varepsilon) \mathbf{u}^\varepsilon) + p^\varepsilon \operatorname{div} \mathbf{u}^\varepsilon = 0.$$

(ii) *A positive renormalisation identity:*

$$(2.11) \quad \partial_t \Pi_\gamma(\rho^\varepsilon | \tilde{\rho}) + \operatorname{div}(h_\gamma(\rho^\varepsilon) \mathbf{u}^\varepsilon) + p^\varepsilon \operatorname{div} \mathbf{u}^\varepsilon = h'_\gamma(\tilde{\rho}) \operatorname{div}(\rho^\varepsilon \mathbf{u}^\varepsilon),$$

where the relative internal energy $\Pi_\gamma(\rho | \tilde{\rho}) := h_\gamma(\rho) - h_\gamma(\tilde{\rho}) - h'_\gamma(\tilde{\rho})(\rho - \tilde{\rho})$ is an affine approximation of h_γ with respect to the hydrostatic density $\tilde{\rho}$.

(iii) *The kinetic energy identity:*

$$(2.12) \quad \partial_t \left(\frac{1}{2} \rho^\varepsilon |\mathbf{u}^\varepsilon|^2 \right) + \operatorname{div} \left(\frac{1}{2} \rho^\varepsilon |\mathbf{u}^\varepsilon|^2 \mathbf{u}^\varepsilon \right) + \frac{1}{\varepsilon^2} \nabla p^\varepsilon \cdot \mathbf{u}^\varepsilon = -\frac{1}{\varepsilon^2} \rho^\varepsilon \nabla \phi \cdot \mathbf{u}^\varepsilon.$$

(iv) *The total energy identity:*

$$(2.13) \quad \partial_t \left(\frac{1}{2} \rho^\varepsilon |\mathbf{u}^\varepsilon|^2 + \frac{1}{\varepsilon^2} \Pi_\gamma(\rho^\varepsilon | \tilde{\rho}) \right) + \operatorname{div} \left(\left(\frac{1}{2} \rho^\varepsilon |\mathbf{u}^\varepsilon|^2 + \frac{1}{\varepsilon^2} h_\gamma(\rho^\varepsilon) + \frac{1}{\varepsilon^2} p^\varepsilon - \frac{1}{\varepsilon^2} h'_\gamma(\tilde{\rho}) \rho^\varepsilon \right) \mathbf{u}^\varepsilon \right) = 0.$$

Proof. Proofs of (2.10)-(2.12) are straightforward; see, e.g. [33] for details in the case of the Navier-Stokes system without source terms. We can obtain (2.13) upon multiplying (2.11) by $\frac{1}{\varepsilon^2}$, adding the resulting equation to (2.12) and making use of the relation (2.7). \square

Remark 2.4. In the case of weak solutions, the identity (2.13) remains as an inequality which represents the decay of mechanical energy. Consequently, throughout the rest of this paper, we will assume that the system (2.1)-(2.3) admits energy stable weak solutions, i.e. weak solutions that satisfy the estimate

$$(2.14) \quad \frac{1}{2} \int_\Omega \rho^\varepsilon |\mathbf{u}^\varepsilon|^2(t, \cdot) d\mathbf{x} + \frac{1}{\varepsilon^2} \int_\Omega \Pi_\gamma(\rho^\varepsilon | \tilde{\rho})(t, \cdot) d\mathbf{x} \leq \frac{1}{2} \int_\Omega \rho_0^\varepsilon |\mathbf{u}_0^\varepsilon|^2 d\mathbf{x} + \frac{1}{\varepsilon^2} \int_\Omega \Pi_\gamma(\rho_0^\varepsilon | \tilde{\rho}) d\mathbf{x}, \quad t \in (0, T) \text{ a.e..}$$

Remark 2.5. The functional

$$\mathcal{E}(\rho^\varepsilon, \mathbf{m}^\varepsilon | \rho, \mathbf{u}) := \frac{1}{2} \int_{\Omega} \rho^\varepsilon \left| \frac{\mathbf{m}^\varepsilon}{\rho^\varepsilon} - \mathbf{u} \right|^2 d\mathbf{x} + \frac{1}{\varepsilon^2} \int_{\Omega} \Pi_\gamma(\rho^\varepsilon | \rho) d\mathbf{x}$$

is called the relative energy or entropy which measures the distance between a pair of solutions $(\rho^\varepsilon, \mathbf{u}^\varepsilon)$ and (ρ, \mathbf{u}) . The relative energy plays a pivotal role in the subsequent analyses carried out.

2.3. Well-Prepared Initial Data and the Anelastic Limit. The anelastic limit of the Euler system (2.1)-(2.2) is obtained by taking limit $\varepsilon \rightarrow 0$ of a sequence of weak solutions $(\rho^\varepsilon, \mathbf{u}^\varepsilon)_{\varepsilon>0}$. For the sake of simplicity, we assume that the given initial data are well-prepared in the following sense.

Definition 2.6 (Well-prepared initial data). An initial datum $(\rho_0^\varepsilon, \mathbf{u}_0^\varepsilon) \in L^\infty(Q_T)^{1+d}$ of the Euler system (2.1)-(2.2) is called well-prepared if

- (i) $\rho_0^\varepsilon > 0$ a.e. in Q_T ;
- (ii) $\rho_0^\varepsilon = \tilde{\rho} + \varepsilon r_0^\varepsilon$, where $\{r_0^\varepsilon\}_{\varepsilon>0} \subset L^\infty(\Omega)$ is uniformly bounded and $r_0^\varepsilon \rightarrow 0$ in $L^2(\Omega)$ as $\varepsilon \rightarrow 0$;
- (iii) $\mathbf{u}_0^\varepsilon \rightarrow \mathbf{U}_0$ in $L^2(\Omega)^d$ as $\varepsilon \rightarrow 0$, with $\operatorname{div}(\tilde{\rho}\mathbf{U}_0) = 0$.

There are many rigorous studies on the anelastic approximation as a singular limit of hydrodynamic models in the literature; see, e.g. [8, 9, 10, 11, 23, 24, 38]. Note that the right hand side of the energy estimate (2.14) remains uniformly bounded, given the initial data $(\rho_0^\varepsilon, \mathbf{u}_0^\varepsilon)$ is well-prepared. Hence, if $(\rho^\varepsilon, \mathbf{u}^\varepsilon)$ is an energy stable weak solution of (2.1)-(2.3) with respect to a well-prepared initial datum, we have the uniform boundedness of the relative energy from the estimate (2.14). The control of the relative internal energy functional Π_γ leads to a strong convergence of the density $\rho^\varepsilon \rightarrow \tilde{\rho}$. Consequently, the uniform bound on the kinetic energy yields a weak-* convergence of the momentum as $\varepsilon \rightarrow 0$. We summarise the essence of anelastic limit in the following theorem and refer the reader to the above cited references for an elaborate treatment.

Theorem 2.7. *Let $(\rho^\varepsilon, \mathbf{m}^\varepsilon)_{\varepsilon>0}$ be a sequence of energy stable weak solutions of the Euler system (2.1)-(2.3) with respect to a sequence of well-prepared initial data $(\rho_0^\varepsilon, \mathbf{m}_0^\varepsilon)_{\varepsilon>0}$. Then the following holds.*

(i) *The relative energy $\mathcal{E}(\rho^\varepsilon, \mathbf{m}^\varepsilon | \tilde{\rho}, \mathbf{U})(t)$ satisfies*

$$(2.15) \quad \lim_{\varepsilon \rightarrow 0} \sup_{t \in (0, T)} \mathcal{E}(\rho^\varepsilon, \mathbf{m}^\varepsilon | \tilde{\rho}, \mathbf{U})(t) = 0;$$

(ii) *$\rho^\varepsilon \rightarrow \tilde{\rho}$ in $L^\infty(0, T; (L^2 + L^{\gamma'})(\Omega))$ as $\varepsilon \rightarrow 0$, with $\gamma' = \min\{2, \gamma\}$;*

(iii) *$\frac{\mathbf{m}^\varepsilon}{\sqrt{\rho^\varepsilon}} \rightarrow \sqrt{\tilde{\rho}}\mathbf{U}$ in $L^\infty(0, T; L^2(\Omega)^d)$ and $\mathbf{m}^\varepsilon \rightarrow \tilde{\rho}\mathbf{U}$ weak-* in $L^\infty(0, T; (L^2 + L^{\bar{\gamma}})(\Omega)^d)$ as $\varepsilon \rightarrow 0$, with $\bar{\gamma} = \min\{\frac{4}{3}, \frac{2\gamma}{\gamma+1}\}$,*

where \mathbf{U} is the solution of the following anelastic Euler system on Q_T :

$$(2.16) \quad \operatorname{div}(\tilde{\rho}\mathbf{U}) = 0,$$

$$(2.17) \quad \partial_t(\tilde{\rho}\mathbf{U}) + \operatorname{div}(\tilde{\rho}\mathbf{U} \otimes \mathbf{U}) + \tilde{\rho}\nabla\pi = \mathbf{0},$$

$$(2.18) \quad \mathbf{U}(0, \cdot) = \mathbf{U}_0, \operatorname{div}(\tilde{\rho}\mathbf{U}_0) = 0.$$

For the subsequent calculations, we note the following result which shows that the stiff terms in the momentum balance (2.2) indeed converges to a term $\tilde{\rho}\nabla\pi$ as $\varepsilon \rightarrow 0$ in the sense of distributions. A discrete counterpart of the same is essential to establish the AP property of the numerical scheme.

Corollary 2.8. *Let $(\rho^\varepsilon, \mathbf{m}^\varepsilon)_{\varepsilon>0}$ be a sequence of energy stable weak solutions of the Euler system (2.1)-(2.3) with respect to a sequence of well-prepared initial data $(\rho_0^\varepsilon, \mathbf{m}_0^\varepsilon)$. Then, as $\varepsilon \rightarrow 0$,*

$$\frac{1}{\varepsilon^2} \iint_{Q_T} (\nabla p^\varepsilon + \rho^\varepsilon \nabla \phi) \cdot \boldsymbol{\psi} d\mathbf{x} dt \rightarrow 0 \text{ for any } \boldsymbol{\psi} \in C_c^\infty([0, T] \times \bar{\Omega}) \text{ with } \operatorname{div}(\tilde{\rho}\boldsymbol{\psi}) = 0.$$

Proof. Let, $\boldsymbol{\psi} \in C_c^\infty([0, T] \times \bar{\Omega})^d$ such that $\operatorname{div}(\tilde{\rho}\boldsymbol{\psi}) = 0$. Adding and subtracting the hydrostatic pressure gradient $\nabla\tilde{p}$ and subsequently recalling the steady state relation (2.6), we obtain

$$\begin{aligned}
(2.19) \quad \frac{1}{\varepsilon^2} \iint_{Q_T} (\nabla p^\varepsilon + \rho^\varepsilon \nabla \phi) \cdot \boldsymbol{\psi} \, d\mathbf{x} \, dt &= \frac{1}{\varepsilon^2} \iint_{Q_T} \nabla(p^\varepsilon - \tilde{p}) \cdot \boldsymbol{\psi} \, d\mathbf{x} \, dt + \frac{1}{\varepsilon^2} \iint_{Q_T} (\rho^\varepsilon - \tilde{\rho}) \nabla \phi \cdot \boldsymbol{\psi} \, d\mathbf{x} \, dt \\
&= -\frac{1}{\varepsilon^2} \iint_{Q_T} (p^\varepsilon - \tilde{p}) \operatorname{div} \boldsymbol{\psi} \, d\mathbf{x} \, dt + \frac{1}{\varepsilon^2} \iint_{Q_T} (\rho^\varepsilon - \tilde{\rho}) \nabla \phi \cdot \boldsymbol{\psi} \, d\mathbf{x} \, dt \\
&= -\frac{\gamma-1}{\varepsilon^2} \iint_{Q_T} \Pi_\gamma(\rho^\varepsilon | \tilde{\rho}) \operatorname{div} \boldsymbol{\psi} \, d\mathbf{x} \, dt - \frac{1}{\varepsilon^2} \iint_{Q_T} \wp'(\tilde{\rho})(\rho^\varepsilon - \tilde{\rho}) \operatorname{div} \boldsymbol{\psi} \, d\mathbf{x} \, dt \\
&\quad - \frac{1}{\varepsilon^2} \iint_{Q_T} (\rho^\varepsilon - \tilde{\rho}) \frac{\nabla \tilde{p}}{\tilde{\rho}} \cdot \boldsymbol{\psi} \, d\mathbf{x} \, dt \\
&= -\frac{\gamma-1}{\varepsilon^2} \iint_{Q_T} \Pi_\gamma(\rho^\varepsilon | \tilde{\rho}) \operatorname{div} \boldsymbol{\psi} \, d\mathbf{x} \, dt - \frac{1}{\varepsilon^2} \iint_{Q_T} (\rho^\varepsilon - \tilde{\rho}) \frac{\wp'(\tilde{\rho})}{\tilde{\rho}} \operatorname{div}(\tilde{\rho}\boldsymbol{\psi}) \, d\mathbf{x} \, dt.
\end{aligned}$$

Note that the first term on right hand side of the above relation converges to 0 as $\varepsilon \rightarrow 0$, following (2.15). The second term on the right hand side vanishes as $\operatorname{div}(\tilde{\rho}\boldsymbol{\psi}) = 0$. \square

2.4. Velocity Stabilisation and A priori Energy Estimates. The present work is aimed to design and analyse a finite volume scheme that is energy stable, well-balanced for the hydrostatic steady state and AP for the anelastic limit. The key to achieve these desirable properties is to add a stabilising term to the convective fluxes appearing in (2.1)-(2.2). Accordingly, we consider the modified system

$$(2.20) \quad \partial_t \rho^\varepsilon + \operatorname{div}(\rho^\varepsilon(\mathbf{u}^\varepsilon - \delta \mathbf{u}^\varepsilon)) = 0,$$

$$(2.21) \quad \partial_t(\rho^\varepsilon \mathbf{u}^\varepsilon) + \operatorname{div}(\rho^\varepsilon \mathbf{u}^\varepsilon \otimes (\mathbf{u}^\varepsilon - \delta \mathbf{u}^\varepsilon)) + \frac{1}{\varepsilon^2} \nabla p^\varepsilon = -\frac{1}{\varepsilon^2} \rho^\varepsilon \nabla \phi.$$

We supplement the above system with the same initial and boundary conditions (2.3). The expression for the stabilisation term $\delta \mathbf{u}^\varepsilon$ will be derived using the total energy balance in such a way that the stability or the decay of mechanical energy of the solutions is ensured; see [1, 2, 15, 16] for analogous considerations for the Euler systems with and without source terms. The implications of the energy stability in terms of the relative energy are multifold. Since the relative energy is defined with respect to the hydrostatic steady state, an adaptation of the same for a finite volume scheme first leads to the well-balancing property. Second, it plays a crucial role in establishing the asymptotic limit $\varepsilon \rightarrow 0$ by providing uniform estimates on the relative internal energy Π_γ and the velocity components with respect to ε . In the following, we establish that the modified system (2.20)-(2.21) is also energy stable and that it admits the same hydrostatic steady states. These observations form the basis for our analysis carried out in Sections 5 and 7. Similar calculations as in Proposition 2.3 readily yields the energy identities satisfied by the velocity stabilised Euler system (2.20)-(2.21).

Proposition 2.9. *The following identities are satisfied by classical solutions of (2.20)-(2.21).*

(i) *A renormalisation identity:*

$$(2.22) \quad \partial_t h_\gamma(\rho^\varepsilon) + \operatorname{div}(h_\gamma(\rho^\varepsilon)(\mathbf{u}^\varepsilon - \delta \mathbf{u}^\varepsilon)) + p^\varepsilon \operatorname{div}(\mathbf{u}^\varepsilon - \delta \mathbf{u}^\varepsilon) = 0.$$

(ii) A positive renormalisation identity:

$$(2.23) \quad \partial_t \Pi_\gamma(\rho^\varepsilon|\tilde{\rho}) + \operatorname{div}(h_\gamma(\rho^\varepsilon)(\mathbf{u}^\varepsilon - \delta\mathbf{u}^\varepsilon)) + p^\varepsilon \operatorname{div}(\mathbf{u}^\varepsilon - \delta\mathbf{u}^\varepsilon) = h'_\gamma(\tilde{\rho}) \operatorname{div}(\rho^\varepsilon(\mathbf{u}^\varepsilon - \delta\mathbf{u}^\varepsilon)).$$

(iii) A kinetic energy identity:

$$(2.24) \quad \partial_t \left(\frac{1}{2} \rho^\varepsilon |\mathbf{u}^\varepsilon|^2 \right) + \operatorname{div} \left(\frac{1}{2} \rho^\varepsilon |\mathbf{u}^\varepsilon|^2 (\mathbf{u}^\varepsilon - \delta\mathbf{u}^\varepsilon) \right) + \frac{1}{\varepsilon^2} \nabla p^\varepsilon \cdot (\mathbf{u}^\varepsilon - \delta\mathbf{u}^\varepsilon) = -\frac{1}{\varepsilon^2} \rho^\varepsilon \nabla \phi \cdot (\mathbf{u}^\varepsilon - \delta\mathbf{u}^\varepsilon) - \frac{1}{\varepsilon^2} \delta\mathbf{u}^\varepsilon \cdot (\nabla p^\varepsilon + \rho^\varepsilon \nabla \phi).$$

(iv) The total energy identity:

$$(2.25) \quad \partial_t \left(\frac{1}{\varepsilon^2} \Pi_\gamma(\rho^\varepsilon|\tilde{\rho}) + \frac{1}{2} \rho^\varepsilon |\mathbf{u}^\varepsilon|^2 \right) + \operatorname{div} \left(\left(\frac{1}{2} \rho^\varepsilon |\mathbf{u}^\varepsilon|^2 + \frac{1}{\varepsilon^2} h_\gamma(\rho^\varepsilon) + \frac{1}{\varepsilon^2} p^\varepsilon - \frac{1}{\varepsilon^2} h'_\gamma(\tilde{\rho}) \rho^\varepsilon \right) (\mathbf{u}^\varepsilon - \delta\mathbf{u}^\varepsilon) \right) = -\frac{1}{\varepsilon^2} \delta\mathbf{u}^\varepsilon \cdot (\nabla p^\varepsilon + \rho^\varepsilon \nabla \phi).$$

Remark 2.10. Thus, at the continuous level, we immediately see that if we formally take

$$(2.26) \quad \delta\mathbf{u}^\varepsilon = \frac{\eta^\varepsilon}{\varepsilon^2} (\nabla p^\varepsilon + \rho^\varepsilon \nabla \phi), \quad \eta^\varepsilon > 0,$$

then we get the energy stability inequality:

$$(2.27) \quad \partial_t \left(\frac{1}{\varepsilon^2} \Pi_\gamma(\rho^\varepsilon|\tilde{\rho}) + \frac{1}{2} \rho^\varepsilon |\mathbf{u}^\varepsilon|^2 \right) + \operatorname{div} \left(\left(\frac{1}{2} \rho^\varepsilon |\mathbf{u}^\varepsilon|^2 + \frac{1}{\varepsilon^2} h_\gamma(\rho^\varepsilon) + \frac{1}{\varepsilon^2} p^\varepsilon - \frac{1}{\varepsilon^2} h'_\gamma(\tilde{\rho}) \rho^\varepsilon \right) (\mathbf{u}^\varepsilon - \delta\mathbf{u}^\varepsilon) \right) \leq 0.$$

2.5. Hydrostatic Steady States of the Velocity Stabilised System. The steady states of the velocity stabilised system (2.20)-(2.21) are given by

$$(2.28) \quad \operatorname{div}(\rho^\varepsilon(\mathbf{u}^\varepsilon - \delta\mathbf{u}^\varepsilon)) = 0,$$

$$(2.29) \quad \operatorname{div}(\rho^\varepsilon \mathbf{u}^\varepsilon \otimes (\mathbf{u}^\varepsilon - \delta\mathbf{u}^\varepsilon)) + \frac{1}{\varepsilon^2} \nabla p^\varepsilon = -\frac{1}{\varepsilon^2} \rho^\varepsilon \nabla \phi.$$

Since we are interested in hydrostatic steady states, we put $\mathbf{u}^\varepsilon = \mathbf{0}$ in the above and readily infer from the momentum equation (2.29) that

$$(2.30) \quad \nabla p^\varepsilon = -\rho^\varepsilon \nabla \phi.$$

Consequently, we get $\delta\mathbf{u}^\varepsilon = \mathbf{0}$ using (2.26). Hence, the mass equation (2.28) implies that the hydrostatic steady state solution $\rho^\varepsilon = \tilde{\rho}$ and $\mathbf{u}^\varepsilon = \mathbf{0}$ of the Euler system (2.1)-(2.2) is also a stationary solution of the modified Euler system (2.20)-(2.21). Note that the velocity stabilisation term $\delta\mathbf{u}^\varepsilon$ is consistent with the steady state in the sense that it vanishes for steady state solutions. Furthermore, to obtain the energy stability of the solutions of the modified system (2.20)-(2.21), we enforce the steady state condition (2.30) also on the boundary of the domain, i.e.

$$(2.31) \quad \nabla p^\varepsilon + \rho^\varepsilon \nabla \phi = \mathbf{0} \text{ on } \partial\Omega.$$

Remark 2.11. Integrating (2.27) on Q_T and using the above boundary conditions yields the following energy stability for any $t \in (0, T)$:

$$(2.32) \quad \frac{1}{2} \int_\Omega \rho^\varepsilon |\mathbf{u}^\varepsilon|^2(t, \cdot) d\mathbf{x} + \frac{1}{\varepsilon^2} \int_\Omega \Pi_\gamma(\rho^\varepsilon(t, \cdot)|\tilde{\rho}) d\mathbf{x} \leq \frac{1}{2} \int_\Omega \rho_0^\varepsilon |\mathbf{u}_0^\varepsilon|^2 d\mathbf{x} + \frac{1}{\varepsilon^2} \int_\Omega \Pi_\gamma(\rho_0^\varepsilon|\tilde{\rho}) d\mathbf{x}.$$

Suppose the initial data is in hydrostatic state, i.e. $\rho_0^\varepsilon = \tilde{\rho}$, $\mathbf{u}_0^\varepsilon = \mathbf{0}$. Since Π_γ is positive and $\Pi_\gamma(a|b) = 0$ if and only if $a = b$ for any $a, b \in \mathbb{R}$, the right hand side of (2.32) vanishes. Since the terms on the left hand side are non-negative, we immediately get $\rho^\varepsilon(t, \cdot) = \tilde{\rho}$ and $\mathbf{u}^\varepsilon(t, \cdot) = \mathbf{0}$ for all $t > 0$. In other words, the stabilised system preserves the hydrostatic steady state, provided

the initial data are hydrostatic. The well-balancing property of our finite volume scheme follows an adaptation of this result that is ensured by the discrete energy stability.

3. SPACE DISCRETISATION AND DISCRETE DIFFERENTIAL OPERATORS

In order to approximate the velocity stabilised Euler system (2.20)-(2.21) in a finite volume framework, we take a computational space-domain $\Omega \subseteq \mathbb{R}^d$ such that the closure of Ω is the union of closed rectangles ($d = 2$) or closed orthogonal parallelepipeds ($d = 3$). In this section, we briefly introduce a discretisation of the domain Ω using a marker and cell (MAC) grid and the corresponding discrete function spaces; see [28, 30, 37] for more details.

3.1. Mesh and Unknowns. A MAC grid is a pair $\mathcal{T} = (\mathcal{M}, \mathcal{E})$, where \mathcal{M} is called the primal mesh which is a partition of $\bar{\Omega}$ consisting of possibly non-uniform closed rectangles ($d = 2$) or parallelepipeds ($d = 3$) and \mathcal{E} is the collection of all edges of the primal mesh cells. For each $\sigma \in \mathcal{E}$, we construct a dual cell D_σ which is the union of half-portions of the primal cells K and L , where $\sigma = \bar{K} \cap \bar{L}$. Furthermore, we decompose \mathcal{E} as $\mathcal{E} = \cup_{i=1}^d \mathcal{E}^{(i)}$, where $\mathcal{E}^{(i)} = \mathcal{E}_{\text{int}}^{(i)} \cup \mathcal{E}_{\text{ext}}^{(i)}$. Here, $\mathcal{E}_{\text{int}}^{(i)}$ and $\mathcal{E}_{\text{ext}}^{(i)}$ are, respectively, the collection of $(d - 1)$ -dimensional internal and external edges that are orthogonal to the i -th unit vector $e^{(i)}$ of the canonical basis of \mathbb{R}^d . We denote by $\mathcal{E}(K)$, the collection of all edges of $K \in \mathcal{M}$ and $\tilde{\mathcal{E}}(D_\sigma)$, the collection of all edges of the dual cell D_σ .

Now, we define a discrete function space $L_{\mathcal{M}}(\Omega) \subset L^\infty(\Omega)$, consisting of scalar valued functions which are piecewise constant on each primal cell $K \in \mathcal{M}$. Analogously, we denote by $\mathbf{H}_{\mathcal{E}}(\Omega) = \prod_{i=1}^d H_{\mathcal{E}}^{(i)}(\Omega)$, the set of vector valued (in \mathbb{R}^d) functions which are constant on each dual cell D_σ for each $\sigma \in \mathcal{E}^{(i)}$, $i = 1, 2, \dots, d$. The space of vector valued functions vanishing on the external edges is denoted as $\mathbf{H}_{\mathcal{E},0}(\Omega) = \prod_{i=1}^d H_{\mathcal{E},0}^{(i)}(\Omega)$, where $H_{\mathcal{E},0}^{(i)}(\Omega)$ contains those elements of $H_{\mathcal{E}}^{(i)}(\Omega)$ which vanish on the external edges. For a primal grid function $q \in L_{\mathcal{M}}(\Omega)$, such that $q = \sum_{K \in \mathcal{M}} q_K \mathcal{X}_K$, and for each $\sigma = K|L \in \cup_{i=1}^d \mathcal{E}_{\text{int}}^{(i)}$, the dual average q_{D_σ} of q over D_σ is defined via the relation

$$(3.1) \quad |D_\sigma|q_{D_\sigma} = |D_{\sigma,K}|q_K + |D_{\sigma,L}|q_L.$$

Remark 3.1. All along the subsequent exposition we have assumed that the dual variables along with the gradients defined on the dual cells vanish on the boundary for the sake of simplicity of performing the analysis. However, we have implemented several other relevant boundary conditions while carrying out various numerical test cases in Section 8.

3.2. Discrete Convection Fluxes and Differential Operators. In this subsection we introduce the discrete convection fluxes and discrete differential operators on the function spaces described above. Let us assume that a discretisation of Ω is done using a MAC grid $\mathcal{T} = (\mathcal{M}, \mathcal{E})$. Construction of the mass flux requires the following technical result which is stated below for convenience and referred to [29, Lemma 2] for proof.

Lemma 3.2. *Let ψ be a strictly convex and continuously differentiable function over an open interval I of \mathbb{R} . If $\rho_K, \rho_L \in I$, then there exists a unique $\rho_{KL} \in \llbracket \rho_K, \rho_L \rrbracket$ such that*

$$(3.2) \quad \psi(\rho_K) + \psi'(\rho_K)(\rho_{KL} - \rho_L) = \psi(\rho_L) + \psi'(\rho_L)(\rho_{KL} - \rho_L), \text{ if } \rho_K \neq \rho_L,$$

and $\rho_{KL} = \rho_K = \rho_L$, otherwise. In particular, for $\wp(\rho) = \rho^\gamma$, and for each $K, L \in \mathcal{M}$, there exists a unique $\rho_{KL} \in \llbracket \rho_K, \rho_L \rrbracket$ such that

$$(3.3) \quad \begin{aligned} \rho_K^\gamma - \rho_L^\gamma &= \rho_{KL} [h'_\gamma(\rho_K) - h'_\gamma(\rho_L)], \text{ if } \rho_K \neq \rho_L, \\ \rho_{KL} &= \rho_K = \rho_L, \text{ otherwise.} \end{aligned}$$

Remark 3.3. In the above lemma and throughout the rest of this paper, we denote by $\llbracket a, b \rrbracket$, the interval $[\min\{a, b\}, \max\{a, b\}]$ for two real numbers a and b .

Definition 3.4. The mass and momentum convection fluxes are defined as follows.

- For each $K \in \mathcal{M}$, and $\sigma \in \mathcal{E}(K)$, the mass convection flux $F_{\sigma,K}: L_{\mathcal{M}}(\Omega) \times \mathbf{H}_{\mathcal{E},0}(\Omega) \rightarrow \mathbb{R}$ is defined by

$$(3.4) \quad F_{\sigma,K}(\rho, \mathbf{u}) := |\sigma| \rho_{\sigma} (u_{\sigma,K} - \delta u_{\sigma,K}), \quad (\rho, \mathbf{u}) \in L_{\mathcal{M}}(\Omega) \times \mathbf{H}_{\mathcal{E},0}(\Omega).$$

Here, $u_{\sigma,K} = u_{\sigma} \mathbf{e}^{(i)} \cdot \boldsymbol{\nu}_{\sigma,K}$ with $\boldsymbol{\nu}_{\sigma,K}$ being the unit vector normal to the edge $\sigma = K|L \in \mathcal{E}_{\text{int}}^{(i)}$ in the direction outward to the cell K . The approximation of the density on each interface $\sigma = K|L \in \mathcal{E}_{\text{int}}^{(i)}$, $i = 1, 2, \dots, d$, is obtained using Lemma 3.2 as $\rho_{\sigma} = \rho_{KL}$, where ρ_{KL} is given by (3.3). The velocity stabilisation term $\delta \mathbf{u} \in \mathbf{H}_{\mathcal{E},0}(\Omega)$ which depends on ρ and the discretised potential ϕ will be specified later.

- For a fixed $i = 1, 2, \dots, d$, for each $\sigma \in \mathcal{E}^{(i)}$, $\epsilon \in \bar{\mathcal{E}}_{D_{\sigma}}$, and $(\rho, \mathbf{u}, v) \in L_{\mathcal{M}}(\Omega) \times \mathbf{H}_{\mathcal{E},0} \times H_{\mathcal{E},0}^{(i)}$, the upwind momentum convection flux is given by the expression

$$(3.5) \quad \sum_{\epsilon \in \bar{\mathcal{E}}(D_{\sigma})} F_{\epsilon,\sigma}(\rho, \mathbf{u}) v_{\epsilon,\text{up}}.$$

Here, $F_{\epsilon,\sigma}(\rho, \mathbf{u})$ is the mass flux across the edge ϵ of the dual cell D_{σ} which is taken to be 0 if $\epsilon \in \mathcal{E}_{\text{ext}}$; otherwise, it is a suitable linear combination of the primal mass convection fluxes at the neighbouring edges with constant coefficients; see, e.g. [30] for more details.

- For any dual face $\epsilon = D_{\sigma}|D_{\sigma'}$ we have $F_{\epsilon,\sigma}(\rho, \mathbf{u}) = -F_{\epsilon,\sigma'}(\rho, \mathbf{u})$. Note that same is true for the primary mass fluxes, i.e. for any $\sigma = K|L$, we have $F_{\sigma,K}(\rho, \mathbf{u}) = -F_{\sigma',K}(\rho, \mathbf{u})$.
- In (3.5), $v_{\epsilon,\text{up}}$ is determined by the following upwind choice:

$$(3.6) \quad v_{\epsilon,\text{up}} := \begin{cases} v_{\sigma}, & F_{\epsilon,\sigma}(\rho, \mathbf{u}) \geq 0, \\ v_{\sigma'}, & \text{otherwise.} \end{cases}$$

Definition 3.5 (Discrete gradient, divergence and Laplacian operators). The discrete gradient operator $\nabla_{\mathcal{E}}: L_{\mathcal{M}}(\Omega) \rightarrow \mathbf{H}_{\mathcal{E},0}(\Omega)$ is defined by the map $q \mapsto \nabla_{\mathcal{E}} q = \left(\partial_{\mathcal{E}}^{(1)} q, \partial_{\mathcal{E}}^{(2)} q, \dots, \partial_{\mathcal{E}}^{(d)} q \right)$, where for each $i = 1, 2, \dots, d$, $\partial_{\mathcal{E}}^{(i)} q$ denotes

$$(3.7) \quad \partial_{\mathcal{E}}^{(i)} q := \sum_{\sigma \in \mathcal{E}_{\text{int}}^{(i)}} (\partial_{\mathcal{E}}^{(i)} q)_{\sigma} \mathcal{X}_{D_{\sigma}}, \quad \text{with } (\partial_{\mathcal{E}}^{(i)} q)_{\sigma} := \frac{|\sigma|}{|D_{\sigma}|} (q_L - q_K) \mathbf{e}^{(i)} \cdot \boldsymbol{\nu}_{\sigma,K}, \quad \sigma = K|L \in \mathcal{E}_{\text{int}}^{(i)}.$$

We set the gradient to zero on the external faces in all the subsequent analysis for the sake of ease. Note that the approximation of the interface values provided by Lemma 3.2 and the definition of discrete gradient (3.7) further implies the following identity for any $q \in L_{\mathcal{M}}(\Omega)$ and $\gamma > 1$:

$$(3.8) \quad (\partial_{\mathcal{E}}^{(i)} q^{\gamma})_{\sigma} = q_{\sigma} (\partial_{\mathcal{E}}^{(i)} h'_{\gamma}(q))_{\sigma}, \quad \sigma \in \mathcal{E}_{\text{int}}^{(i)}, \quad i = 1, 2, \dots, d.$$

The discrete divergence operator $\text{div}_{\mathcal{M}}: L_{\mathcal{M}}(\Omega) \times \mathbf{H}_{\mathcal{E},0}(\Omega) \rightarrow L_{\mathcal{M}}(\Omega)$ is defined as $(q, \mathbf{v}) \mapsto \text{div}_{\mathcal{M}}(q\mathbf{v}) = \sum_{K \in \mathcal{M}} (\text{div}_{\mathcal{M}}(q\mathbf{v}))_K \mathcal{X}_K$, where for each $K \in \mathcal{M}$, $(\text{div}_{\mathcal{M}}\mathbf{v})_K$ denotes

$$(3.9) \quad (\text{div}_{\mathcal{M}}(q\mathbf{v}))_K := \frac{1}{|K|} \sum_{\sigma \in \mathcal{E}(K)} |\sigma| q_{\sigma} v_{\sigma,K},$$

with q_σ being defined as in Lemma 3.2. In particular, for any $\mathbf{v} \in \mathbf{H}_{\mathcal{E},0}(\Omega)$, we have $\operatorname{div}_{\mathcal{M}} \mathbf{v} = \sum_{K \in \mathcal{M}} (\operatorname{div}_{\mathcal{M}} \mathbf{v})_K \mathcal{X}_K \in L_{\mathcal{M}}(\Omega)$, where

$$(3.10) \quad (\operatorname{div}_{\mathcal{M}} \mathbf{v})_K := \frac{1}{|K|} \sum_{\sigma \in \mathcal{E}(K)} |\sigma| v_{\sigma,K}.$$

Finally, the discrete Laplacian operator $\Delta_{\mathcal{M}}: L_{\mathcal{M}}(\Omega) \rightarrow L_{\mathcal{M}}(\Omega)$ is defined via the map $q \mapsto \Delta_{\mathcal{M}} q = \sum_{K \in \mathcal{M}} (\Delta_{\mathcal{M}} q)_K \mathcal{X}_K \in L_{\mathcal{M}}(\Omega)$, where

$$(3.11) \quad (\Delta_{\mathcal{M}} q)_K := (\operatorname{div}_{\mathcal{M}}(\nabla_{\mathcal{E}} q))_K, \quad \forall K \in \mathcal{M}.$$

Proposition 3.6 (Div-grad duality). *For any $(p, q, \mathbf{v}) \in L_{\mathcal{M}}(\Omega) \times L_{\mathcal{M}}(\Omega) \times \mathbf{H}_{\mathcal{E},0}(\Omega)$, the following ‘gradient-divergence duality’ holds for the discrete gradient and divergence operators:*

$$(3.12) \quad \sum_{K \in \mathcal{M}} |K| p_K (\operatorname{div}_{\mathcal{M}}(q\mathbf{v}))_K + \sum_{i=1}^d \sum_{\sigma \in \mathcal{E}_{\text{int}}^{(i)}} |D_\sigma| q_\sigma (\partial_{\mathcal{E}}^{(i)} p)_\sigma v_\sigma = 0.$$

In particular for $q \equiv 1$, and any $(p, \mathbf{v}) \in L_{\mathcal{M}}(\Omega) \times \mathbf{H}_{\mathcal{E},0}(\Omega)$, we have

$$(3.13) \quad \sum_{K \in \mathcal{M}} |K| p_K (\operatorname{div}_{\mathcal{M}} \mathbf{v})_K + \sum_{i=1}^d \sum_{\sigma \in \mathcal{E}_{\text{int}}^{(i)}} |D_\sigma| (\partial_{\mathcal{E}}^{(i)} p)_\sigma v_\sigma = 0.$$

4. THE FINITE VOLUME SCHEME

4.1. A Semi-Implicit Scheme. Based on the finite volume discretisation and the corresponding discrete operators defined in the previous section we now introduce a semi-implicit scheme for the system (2.20)-(2.21).

For the given potential ϕ , the corresponding discrete hydrostatic density $\tilde{\rho}$ is obtained as the cell average on each control volume in the collection of primal cells \mathcal{M} . Accordingly, by a slight abuse of notation, $\tilde{\rho} = \sum_{K \in \mathcal{M}} \tilde{\rho}_K \mathcal{X}_K \in L_{\mathcal{M}}(\Omega)$ denotes the discrete hydrostatic density, where

$$(4.1) \quad \tilde{\rho}_K := \frac{1}{|K|} \int_K \tilde{\rho}(\mathbf{x}) d\mathbf{x} = \frac{1}{|K|} \int_K \left(\frac{\gamma-1}{\gamma} (C(m_0) - \phi(\mathbf{x})) \right)^{\frac{1}{\gamma-1}} d\mathbf{x}, \quad \forall K \in \mathcal{M},$$

following the relations (2.7) and (2.8). Similarly, $\phi = \sum_{K \in \mathcal{M}} \phi_K \mathcal{X}_K \in L_{\mathcal{M}}(\Omega)$ denotes the discrete approximation of the smooth potential ϕ given by

$$(4.2) \quad \phi_K := C(m_0) - h'_\gamma(\tilde{\rho}_K), \quad \forall K \in \mathcal{M},$$

following (2.7).

Let $\delta t > 0$ be a constant time-step. An approximate solution $(\rho^n, \mathbf{u}^n) \in L_{\mathcal{M}}(\Omega) \times \mathbf{H}_{\mathcal{E},0}(\Omega)$ to the stabilised Euler system (2.20)-(2.21) at time $t_n = n\delta t$, for $1 \leq n \leq N = \lfloor \frac{T}{\delta t} \rfloor$, is computed inductively by the following semi-implicit scheme:

$$(4.3) \quad \frac{1}{\delta t} (\rho_K^{n+1} - \rho_K^n) + \frac{1}{|K|} \sum_{\sigma \in \mathcal{E}(K)} F_{\sigma,K}(\rho^{n+1}, \mathbf{u}^n) = 0, \quad \forall K \in \mathcal{M},$$

$$(4.4) \quad \frac{1}{\delta t} (\rho_{D_\sigma}^{n+1} u_\sigma^{n+1} - \rho_{D_\sigma}^n u_\sigma^n) + \frac{1}{|D_\sigma|} \sum_{\epsilon \in \mathcal{E}(D_\sigma)} F_{\epsilon,\sigma}(\rho^{n+1}, \mathbf{u}^n) u_{\epsilon,\text{up}}^n \\ + \frac{1}{\epsilon^2} (\partial_{\mathcal{E}}^{(i)} p^{n+1})_\sigma = -\frac{1}{\epsilon^2} \rho_\sigma^{n+1} (\partial_{\mathcal{E}}^{(i)} \phi)_\sigma, \quad \forall \sigma \in \mathcal{E}_{\text{int}}^{(i)}, \quad i = 1, 2, \dots, d.$$

We now define the implicit momentum stabilisation term present in the mass flux, cf. Section 3, in accordance with the energy stability analysis as a discrete analogue of (2.26), i.e.

$$(4.5) \quad \delta u_\sigma^{n+1} := \frac{\eta \delta t}{\varepsilon^2} \left[(\partial_{\mathcal{E}}^{(i)} p^{n+1})_\sigma + \rho_\sigma^{n+1} (\partial_{\mathcal{E}}^{(i)} \phi)_\sigma \right].$$

The implicit density term appearing on the right hand side of (4.4) for each $\sigma \in \mathcal{E}_{\text{int}}^{(i)}$, $\sigma = K|L$, is also determined using Lemma 3.2.

Remark 4.1. Note that the implicit density term on the interfaces appearing in the source term is consistent with the mass and momentum fluxes. As we shall see in the subsequent analyses, this feature enables us to obtain the discrete counterpart of the a priori energy estimates in Proposition 2.9, which yields the scheme's stability and finally leads to a consistent discretisation of the anelastic Euler system in the asymptotic limit. In addition, the same interface approximation of the density ensures that the scheme exactly satisfies a discrete analogue of the hydrostatic steady state (2.6).

Remark 4.2. The proposed velocity stabilised scheme (4.3)-(4.4) is closely related to the so-called non-incremental projection schemes [12]. Consequently, the scheme remains first-order accurate. Nonetheless, we validate by a numerical experiment in Subsection 8.6 that the order of accuracy is uniform in ε .

Averaging the mass balance (4.3) over dual cells, we obtain the following mass balance on each dual cell D_σ using the relation between the primal and dual convection fluxes as described in Definition 3.4:

$$(4.6) \quad \frac{1}{\delta t} (\rho_{D_\sigma}^{n+1} - \rho_{D_\sigma}^n) + \frac{1}{|D_\sigma|} \sum_{\epsilon \in \tilde{\mathcal{E}}(D_\sigma)} F_{\epsilon, \sigma}(\rho^{n+1}, \mathbf{u}^n) = 0.$$

The discrete momentum update (4.4) and the dual mass balance (4.6) together yields the following update of the velocity components:

$$(4.7) \quad \frac{u_\sigma^{n+1} - u_\sigma^n}{\delta t} - \frac{1}{|D_\sigma|} \sum_{\epsilon \in \tilde{\mathcal{E}}(D_\sigma)} F_{\epsilon, \sigma}(\rho^{n+1}, \mathbf{u}^n) - \frac{u_\sigma^n - u_\sigma^n}{\rho_{D_\sigma}^{n+1}} + \frac{1}{\varepsilon^2} \frac{1}{\rho_{D_\sigma}^{n+1}} \left((\partial_{\mathcal{E}}^{(i)} p^{n+1})_\sigma + \rho_\sigma^{n+1} (\partial_{\mathcal{E}}^{(i)} \phi)_\sigma \right) = 0.$$

Here, and throughout rest of the paper, $x^\pm = \frac{1}{2}(|x| \pm x)$ denotes the positive and negative parts of a real number x so that $x = x^+ - x^-$ with $x^\pm \geq 0$.

4.2. Initialisation of the scheme. The initial approximations at $t_0 = 0$ is given by the cell averages of the initial data, i.e.

$$(4.8) \quad (\rho^\varepsilon)_K^0 = \frac{1}{|K|} \int_K \rho_0^\varepsilon(\mathbf{x}) d\mathbf{x}, \quad \forall K \in \mathcal{M},$$

$$(4.9) \quad (u^\varepsilon)_\sigma^0 = \frac{1}{|D_\sigma|} \int_{D_\sigma} u_0^{\varepsilon, (i)}(\mathbf{x}) d\mathbf{x}, \quad \forall \sigma \in \mathcal{E}_{\text{int}}^{(i)}.$$

The following estimates are direct consequences of the well-prepared initial datum and its discretisation.

Lemma 4.3. *Let the initial data $(\rho_0^\varepsilon, \mathbf{u}_0^\varepsilon)$ be well-prepared in the sense of Definition 2.6. Then,*

(i) $(\rho^\varepsilon)^0 \in L_{\mathcal{M}}(\Omega)$ satisfies the estimate

$$(4.10) \quad \frac{1}{\varepsilon} \max_{K \in \mathcal{M}} |\rho_K^0 - \tilde{\rho}_K| \leq M(\varepsilon),$$

where $M(\varepsilon) \rightarrow 0$ as $\varepsilon \rightarrow 0$;

(ii) $\{(\mathbf{u}^\varepsilon)^0\}_{\varepsilon>0} \subset \mathbf{H}_{\mathcal{E},0}(\Omega)$ is uniformly bounded.

Remark 4.4. For the sake of brevity, we shall omit ε and denote the discretised initial data as $(\rho^0, \mathbf{u}^0) \in L_{\mathcal{M}}(\Omega) \times \mathbf{H}_{\mathcal{E},0}(\Omega)$ in the subsequent analysis carried out in this section.

4.3. Existence of a Numerical Solution. Having defined the finite volume scheme (4.3)-(4.4), we now proceed to establish its key features. Our first result is regarding the existence and positivity of the density given by the semi-implicit mass update (4.3) for a given data $(\rho^n, \mathbf{u}^n) \in L_{\mathcal{M}}(\Omega) \times \mathbf{H}_{\mathcal{E},0}(\Omega)$ with $\rho^n > 0$ on Ω . Since (4.3) leads to a nonlinear equation for ρ^{n+1} , we make use of a few results from topological degree theory in finite dimensions [14] to establish the existence of a positive solution.

Theorem 4.5. *Let $(\rho^n, \mathbf{u}^n) \in L_{\mathcal{M}}(\Omega) \times \mathbf{H}_{\mathcal{E},0}(\Omega)$ be such that $\rho^n > 0$ on Ω . Then there exists a time-step $\delta t_{\mathcal{T},\Omega}^n > 0$ depending only upon ρ^n , the space discretisation \mathcal{T} , and the domain Ω , such that for any $0 < \delta t \leq \delta t_{\mathcal{T},\Omega}^n$, the updates (4.3)-(4.4) admits a solution $(\rho^{n+1}, \mathbf{u}^{n+1}) \in L_{\mathcal{M}}(\Omega) \times \mathbf{H}_{\mathcal{E},0}(\Omega)$ such that $\rho^{n+1} > 0$.*

Proof. Let $C_{\mathcal{M},\Omega}^n$ be a positive constant defined as

$$(4.11) \quad C_{\mathcal{M},\Omega}^n := |\Omega| \frac{\max_{K \in \mathcal{M}} \{\rho_K^n\}}{\min_{K \in \mathcal{M}} \{|K|\}}.$$

We further define $\Lambda_{\mathcal{M},\Omega}^n(\tilde{\rho}) > 0$ as

$$(4.12) \quad \Lambda_{\mathcal{M},\Omega}^n(\tilde{\rho}) := (C_{\mathcal{M},\Omega}^n)^\gamma + C_{\mathcal{M},\Omega}^n \max_{K \in \mathcal{M}} |h'_\gamma(\tilde{\rho}_K)|.$$

Now, we choose a time-step $\delta t_{\mathcal{T},\Omega}^n > 0$ so that

$$(4.13) \quad \delta t_{\mathcal{T},\Omega}^n \max_{K \in \mathcal{M}} \{\partial K\} \left(C_{\mathcal{M}} \max_{\sigma \in \mathcal{E}_{\text{int}}} |u_\sigma^n| + \frac{1}{\varepsilon} \sqrt{2\eta C_{\mathcal{T}} \Lambda_{\mathcal{M},\Omega}^n(\tilde{\rho})} \right) < \min\{1, \zeta^n\},$$

where $C_{\mathcal{M}} = \max_{K \in \mathcal{M}} \{\frac{1}{|K|}\}$, $C_{\mathcal{T}} = C_{\mathcal{M}} \max_{\sigma \in \mathcal{E}_{\text{int}}} \{\frac{1}{|D_\sigma|}\}$ and $\zeta^n = \frac{\min_{K \in \mathcal{M}} \{\rho_K^n\}}{3C_{\mathcal{M},\Omega}^n}$. The constant $\eta > 0$ is taken as $\eta = \eta_1 \max_{\sigma \in \mathcal{E}_{\text{int}}} \{\frac{1}{\rho_{D_\sigma}^n}\}$ with $\eta_1 > 3/2$. Let $C > C_{\mathcal{M},\Omega}^n$ and let us define an open bounded set $V \subset L_{\mathcal{M}}(\Omega)$ via

$$(4.14) \quad V := \{\rho \in L_{\mathcal{M}}(\Omega) : 0 < \rho_K < C, \forall K \in \mathcal{M}\}.$$

For any $0 < \delta t \leq \delta t_{\mathcal{T},\Omega}^n$, let us introduce a function $H: [0, 1] \times L_{\mathcal{M}}(\Omega) \rightarrow L_{\mathcal{M}}(\Omega)$ such that

$$\begin{aligned} (\lambda, \rho) &\mapsto \sum_{K \in \mathcal{M}} H(\lambda, \rho)_K \mathcal{X}_K, \quad \forall (\lambda, \rho) \in [0, 1] \times L_{\mathcal{M}}(\Omega), \\ H(\lambda, \rho)_K &:= (\rho_K - \rho_K^n) + \frac{\lambda \delta t}{|K|} \sum_{\sigma \in \mathcal{E}(K)} F_{\sigma,K}(\rho, \mathbf{u}^n), \quad \forall K \in \mathcal{M}. \end{aligned}$$

Note that $H(\lambda, \cdot)$ is a homotopy connecting $H(0, \cdot)$ and $H(1, \cdot)$. We first show that $H(\lambda, \cdot) \neq 0$ on ∂V , for any $\lambda \in [0, 1]$, which in turn would imply that $H(\lambda, \cdot)$ has a non-zero topological degree with respect to V . On the contrary, let us assume that $H(\lambda, \rho^\lambda) = 0$ for some $\lambda \in [0, 1]$ and $\rho^\lambda \in \partial V$. So we have that

$$(4.15) \quad (\rho_K^\lambda - \rho_K^n) + \frac{\lambda \delta t}{|K|} \sum_{\sigma \in \mathcal{E}(K)} F_{\sigma,K}(\rho^\lambda, \mathbf{u}^n) = 0, \quad \forall K \in \mathcal{M}.$$

Since $\rho^\lambda \in \partial V \subset \bar{V}$, taking sum over all $K \in \mathcal{M}$ in (4.15), we have,

$$(4.16) \quad 0 \leq \rho_K^\lambda \leq C_{\mathcal{M},\Omega}^n < C, \quad \forall K \in \mathcal{M}.$$

Now, for a time-step $0 < \delta t \leq \delta t_{\mathcal{T},\Omega}^n$, we further have from (4.13) and (4.16) that for each $K \in \mathcal{M}$

$$(4.17) \quad \frac{1}{3}\rho_K^n > \frac{\lambda\delta t}{|K|} \sum_{\sigma \in \mathcal{E}(K)} |F_{\sigma,K}(\rho^\lambda, u^n)|,$$

from which, taking (4.15) into account we have,

$$(4.18) \quad \frac{1}{2}\rho_K^\lambda - \frac{\lambda\delta t}{|K|} \sum_{\sigma \in \mathcal{E}(K)} |F_{\sigma,K}(\rho^\lambda, u^n)| > 0, \quad \forall K \in \mathcal{M}.$$

From (4.16) and (4.18) we have

$$(4.19) \quad 0 < \rho_K^\lambda < C, \quad \forall K \in \mathcal{M},$$

which contradicts the assumption that $\rho^\lambda \in \partial V$. Hence, we have that for any $\lambda \in [0, 1]$, $H(\lambda, \cdot) \neq 0$ on ∂V which implies that $\deg H(1, \cdot) = \deg H(0, \cdot)$ on V . Since $\deg H(0, \cdot) \neq 0$, we conclude that $H(1, \cdot)$ has a zero in V . In other words, there exists a solution $\rho^{n+1} \in \mathcal{M}(\Omega)$ to the mass update (4.3) satisfying $\rho^{n+1} > 0$. Subsequently, the updated velocity can be explicitly determined from (4.4). \square

5. ENERGY STABILITY AND WELL-BALANCING

In this section we establish the nonlinear energy stability of the semi-implicit scheme developed in Section 4.1. To this end, we first prove the discrete counter parts of the energy balances stated in Proposition 2.3.

5.1. Internal Energy Balance. The following lemma gives the discrete internal energy balance for the scheme (4.3)-(4.4).

Lemma 5.1 (Renormalisation identify). *Let $(\rho^{n+1}, \mathbf{u}^{n+1}) \in L_{\mathcal{M}}(\Omega) \times \mathbf{H}_{\varepsilon,0}(\Omega)$ be a solution to the semi-implicit scheme (4.3)-(4.4). Then for all $K \in \mathcal{M}$, the following holds:*

$$(5.1) \quad \frac{|K|}{\delta t} (h_\gamma(\rho_K^{n+1}) - h_\gamma(\rho_K^n)) + h'_\gamma(\rho_K^{n+1}) \sum_{\sigma \in \mathcal{E}(K)} F_{\sigma,K}(\rho^{n+1}, \mathbf{u}^n) + \mathcal{R}_{K,\delta t}^{n+1,n} = 0,$$

where $\mathcal{R}_{K,\delta t}^{n+1,n} \geq 0$.

Proof. Multiplying the discrete mass update (4.3) by $|K|h'_\gamma(\rho_K^{n+1})$ and using a second-order Taylor expansion yields

$$(5.2) \quad \begin{aligned} 0 &= \frac{|K|}{\delta t} h'_\gamma(\rho_K^{n+1})(\rho_K^{n+1} - \rho_K^n) + h'_\gamma(\rho_K^{n+1}) \sum_{\sigma \in \mathcal{E}(K)} F_{\sigma,K}(\rho^{n+1}, \mathbf{u}^n) \\ &= \frac{|K|}{\delta t} (h'_\gamma(\rho_K^{n+1}) - h'_\gamma(\rho_K^n)) + h'_\gamma(\rho_K^{n+1}) \sum_{\sigma \in \mathcal{E}(K)} F_{\sigma,K}(\rho^{n+1}, \mathbf{u}^n) \\ &\quad + \frac{1}{2} \frac{|K|}{\delta t} h''_\gamma(\bar{\rho}_K^{n+\frac{1}{2}})(\rho_K^{n+1} - \rho_K^n)^2, \end{aligned}$$

where $\bar{\rho}_K^{n+\frac{1}{2}} \in [\rho_K^{n+1}, \rho_K^n]$. The non-negativity of the remainder term $\mathcal{R}_{K,\delta t}^{n+1,n}$ follows from the convexity of h_γ . \square

The following discrete relative internal energy balance follows as an immediate corollary to Lemma 5.1.

Corollary 5.2 (Positive renormalisation identity). *Let $(\rho^{n+1}, \mathbf{u}^{n+1}) \in L_{\mathcal{M}}(\Omega) \times \mathbf{H}_{\mathcal{E},0}(\Omega)$ be a solution to the semi-implicit scheme (4.3)-(4.4). Then for all $K \in \mathcal{M}$, the following holds:*

$$(5.3) \quad \begin{aligned} & \frac{|K|}{\varepsilon^2 \delta t} (\Pi_{\gamma}(\rho_K^{n+1} | \tilde{\rho}_K) - \Pi_{\gamma}(\rho_K^n | \tilde{\rho}_K)) + \frac{1}{\varepsilon^2} h'_{\gamma}(\rho_K^{n+1}) \sum_{\sigma \in \mathcal{E}(K)} F_{\sigma,K}(\rho^{n+1}, \mathbf{u}^n) + \mathcal{R}_{K,\delta t}^{n+1,n} \\ & = \frac{1}{\varepsilon^2} h'_{\gamma}(\tilde{\rho}_K) \sum_{\sigma \in \mathcal{E}(K)} F_{\sigma,K}(\rho^{n+1}, \mathbf{u}^n), \end{aligned}$$

where $\mathcal{R}_{K,\delta t}^{n+1,n} \geq 0$.

5.2. Kinetic Energy Estimate. In the following lemma we establish a discrete kinetic energy estimate for the numerical scheme.

Lemma 5.3 (Discrete kinetic energy identity). *Any solution to the system (4.3)-(4.4) satisfies the following equality for $1 \leq i \leq d$, $\sigma \in \mathcal{E}_{\text{int}}^{(i)}$ and $0 \leq n \leq N-1$:*

$$(5.4) \quad \begin{aligned} & \frac{1}{2} \frac{|D_{\sigma}|}{\delta t} (\rho_{D_{\sigma}}^{n+1} (u_{\sigma}^{n+1})^2 - \rho_{D_{\sigma}}^n (u_{\sigma}^n)^2) + \sum_{\epsilon \in \tilde{\mathcal{E}}(D_{\sigma})} F_{\epsilon,\sigma}(\rho^{n+1}, \mathbf{u}^n) \frac{|u_{\epsilon}^n|^2}{2} + \frac{1}{\varepsilon^2} |D_{\sigma}| (\partial_{\mathcal{E}}^{(i)} p^{n+1})_{\sigma} u_{\sigma}^n \\ & + \mathcal{R}_{\sigma,\delta t}^{n+1} = -\frac{1}{\varepsilon^2} |D_{\sigma}| \rho_{\sigma}^{n+1} (\partial_{\mathcal{E}}^{(i)} \phi)_{\sigma} u_{\sigma}^n, \end{aligned}$$

where the remainder term $\mathcal{R}_{\sigma,\delta t}^{n+1}$ is defined by

$$(5.5) \quad \mathcal{R}_{\sigma,\delta t}^{n+1} = -\frac{|D_{\sigma}|}{2\delta t} \rho_{D_{\sigma}}^{n+1} (u_{\sigma}^{n+1} - u_{\sigma}^n)^2 + \sum_{\substack{\epsilon \in \tilde{\mathcal{E}}(D_{\sigma}) \\ \epsilon = D_{\sigma} | D_{\sigma'}}} F_{\epsilon,\sigma}(\rho^{n+1}, \mathbf{u}^n) - \frac{(u_{\sigma}^n - u_{\sigma'}^n)^2}{2}.$$

Proof. Multiplying the momentum balance equation (4.4) by $|D_{\sigma}| u_{\sigma}^n$ and using the dual mass balance (4.6) yields the identity. \square

5.3. Discrete Total Energy Estimate. Following the discrete relative internal energy balance (5.3) and the discrete kinetic energy balance (5.4), we now proceed to prove a discrete counterpart of the energy stability (2.32) in the following theorem.

Theorem 5.4 (Total energy balance). *Any solution to the system (4.3)-(4.4) satisfies the following energy inequality:*

$$(5.6) \quad \frac{1}{\varepsilon^2} \sum_{K \in \mathcal{M}} |K| \Pi_{\gamma}(\rho_K^{n+1} | \tilde{\rho}_K) + \sum_{\sigma \in \mathcal{E}_{\text{int}}} |D_{\sigma}| \frac{1}{2} \rho_{D_{\sigma}}^{n+1} (u_{\sigma}^{n+1})^2 \leq \frac{1}{\varepsilon^2} \sum_{K \in \mathcal{M}} |K| \Pi_{\gamma}(\rho_K^n | \tilde{\rho}_K) + \sum_{\sigma \in \mathcal{E}_{\text{int}}} |D_{\sigma}| \frac{1}{2} \rho_{D_{\sigma}}^n (u_{\sigma}^n)^2,$$

under the time-step restrictions $\forall \sigma \in \mathcal{E}_{\text{int}}^{(i)}$, $1 \leq i \leq d$:

$$(5.7) \quad \frac{\delta t}{|D_{\sigma}|} \sum_{\epsilon \in \tilde{\mathcal{E}}(D_{\sigma})} \frac{F_{\epsilon,\sigma}(\rho^{n+1}, \mathbf{u}^n)^-}{\rho_{D_{\sigma}}^{n+1}} \leq \frac{1}{2},$$

and the condition on η such that $\forall \sigma \in \mathcal{E}_{\text{int}}^{(i)}$, $1 \leq i \leq d$:

$$(5.8) \quad \eta \geq \frac{1}{\rho_{D_{\sigma}}^{n+1}}.$$

Proof. We take sums over $K \in \mathcal{M}$ in (5.3) and over $\sigma \in \mathcal{E}_{\text{int}}$ in (5.4). Upon adding the resulting expressions and recalling (3.8), (5.16) and the discrete duality (3.12) we obtain

$$(5.9) \quad \begin{aligned} & \frac{1}{\varepsilon^2 \delta t} \sum_{K \in \mathcal{M}} |K| \left(\Pi_\gamma(\rho_K^{n+1} | \tilde{\rho}_K) - \Pi_\gamma(\rho_K^n | \tilde{\rho}_K) \right) + \sum_{\sigma \in \mathcal{E}_{\text{int}}} \frac{1}{2} \frac{|D_\sigma|}{\delta t} \left(\rho_{D_\sigma}^{n+1} (u_\sigma^{n+1})^2 - \rho_{D_\sigma}^n (u_\sigma^n)^2 \right) \\ & + \mathcal{R}_{\mathcal{M}, \delta t}^{n+1} + \mathcal{R}_{\mathcal{E}, \delta t}^{n+1} = -\frac{\eta \delta t}{\varepsilon^4} \sum_{i=1}^d \sum_{\sigma \in \mathcal{E}_{\text{int}}^{(i)}} |D_\sigma| \left((\partial_\mathcal{E}^{(i)} p^{n+1})_\sigma + \rho_\sigma^{n+1} (\partial_\mathcal{E}^{(i)} \phi)_\sigma \right)^2. \end{aligned}$$

Here, the global remainder terms $\mathcal{R}_{\mathcal{M}, \delta t}^{n+1}$ and $\mathcal{R}_{\mathcal{E}, \delta t}^{n+1}$ are obtained by summing the local remainders $\mathcal{R}_{K, \delta t}^{n+1}$ and $\mathcal{R}_{\sigma, \delta t}^{n+1}$, respectively. Since $\mathcal{R}_{\mathcal{M}, \delta t}^{n+1}$ is non-negative unconditionally, the required stability estimate (5.6) follows from (5.9) once we enforce the non-negativity of $\mathcal{R}_{\mathcal{E}, \delta t}^{n+1}$. To this end, we use the elementary inequality $(a+b)^2 \leq 2a^2 + 2b^2$, $a, b \in \mathbb{R}$, in the velocity update (4.7) to yield

$$(5.10) \quad \begin{aligned} \frac{1}{2} \rho_{D_\sigma}^{n+1} |u_\sigma^{n+1} - u_\sigma^n|^2 & \leq \frac{(\delta t)^2}{|D_\sigma|^2 \rho_{D_\sigma}^{n+1}} \left| - \sum_{\epsilon \in \tilde{\mathcal{E}}(D_\sigma)} (u_{\sigma'}^n - u_\sigma^n) F_{\epsilon, \sigma}(\rho^{n+1}, \mathbf{u}^n)^- \right|^2 \\ & + \frac{(\delta t)^2}{\varepsilon^4 \rho_{D_\sigma}^{n+1}} \left((\partial_\mathcal{E}^{(i)} p^{n+1})_\sigma + \rho_\sigma^{n+1} (\partial_\mathcal{E}^{(i)} \phi)_\sigma \right)^2. \end{aligned}$$

Upon an application of the Cauchy-Schwarz inequality, the first term on the right hand side of (5.10) yields

$$(5.11) \quad \begin{aligned} \left| - \sum_{\epsilon \in \tilde{\mathcal{E}}(D_\sigma)} (u_{\sigma'}^n - u_\sigma^n) F_{\epsilon, \sigma}(\rho^{n+1}, \mathbf{u}^n)^- \right|^2 & \leq \left(\sum_{\epsilon \in \tilde{\mathcal{E}}(D_\sigma)} \frac{F_{\epsilon, \sigma}(\rho^{n+1}, \mathbf{u}^n)^-}{\rho_{D_\sigma}^{n+1}} \right) \\ & \times \left(\sum_{\substack{\epsilon \in \tilde{\mathcal{E}}(D_\sigma) \\ \epsilon = D_\sigma | D_{\sigma'}}} F_{\epsilon, \sigma}(\rho^{n+1}, \mathbf{u}^n)^- (u_\sigma^n - u_{\sigma'}^n)^2 \right). \end{aligned}$$

Using the above inequality and grouping the like-terms on the right hand sides of (5.10)-(5.11), we finally obtain from (5.9), cf. also [1, 15], the following inequality:

$$(5.12) \quad \begin{aligned} & \frac{1}{\varepsilon^2 \delta t} \sum_{K \in \mathcal{M}} |K| \left(\Pi_\gamma(\rho_K^{n+1}) - \Pi_\gamma(\rho_K^n) \right) + \sum_{\sigma \in \mathcal{E}_{\text{int}}} \frac{1}{2} \frac{|D_\sigma|}{\delta t} \left(\rho_{D_\sigma}^{n+1} (u_\sigma^{n+1})^2 - \rho_{D_\sigma}^n (u_\sigma^n)^2 \right) \\ & + \frac{\delta t}{\varepsilon^4} \sum_{i=1}^d \sum_{\sigma \in \mathcal{E}_{\text{int}}^{(i)}} |D_\sigma| \left(\eta - \frac{1}{\rho_{D_\sigma}^{n+1}} \right) \left((\partial_\mathcal{E}^{(i)} p^{n+1})_\sigma + \rho_\sigma^{n+1} (\partial_\mathcal{E}^{(i)} \phi)_\sigma \right)^2 \\ & \leq \sum_{\sigma \in \mathcal{E}_{\text{int}}} \left(\frac{\delta t}{|D_\sigma|} \sum_{\epsilon \in \tilde{\mathcal{E}}(D_\sigma)} \frac{F_{\epsilon, \sigma}(\rho^{n+1}, \mathbf{u}^n)^-}{\rho_{D_\sigma}^{n+1}} - \frac{1}{2} \right) \left(\sum_{\substack{\epsilon \in \tilde{\mathcal{E}}(D_\sigma) \\ \epsilon = D_\sigma | D_{\sigma'}}} F_{\epsilon, \sigma}(\rho^{n+1}, \mathbf{u}^n)^- (u_\sigma^n - u_{\sigma'}^n)^2 \right). \end{aligned}$$

The third term on the left hand side of the above estimate remains non-negative given that the parameter η satisfies the condition (5.8), whereas the right hand side remains non-positive under the time-step restriction (5.7). \square

Remark 5.5. For analogous treatments on momentum and velocity stabilised schemes in the context of the shallow water and barotropic Euler systems without source terms we refer to [1, 15, 16].

Remark 5.6. Note that the stability conditions (5.7) and (5.8) are implicit in nature as they involve ρ^{n+1} . Nevertheless, proceeding as in [1, 16], we can obtain a sufficient condition on the time-step which satisfies the requirement (5.7) and in addition yields

$$(5.13) \quad \frac{\rho_{D_\sigma}^n}{\rho_{D_\sigma}^{n+1}} \leq \frac{3}{2},$$

from the dual mass balance (3.1). Note that (5.13) indeed enables us to make an explicit choice of η as $\eta = \eta_1 / \rho_{D_\sigma}^n$ at each interface σ , where $\eta_1 > 3/2$.

5.4. Well-Balancing Property of the Semi-implicit Scheme. In this section we discuss in detail the well-balancing property of the semi-implicit scheme (4.3)-(4.4). Using the discrete relative energy estimate (5.6) we show that the scheme exactly satisfies and preserves a discrete form of the hydrostatic steady state.

Upon direct verification we can immediately observe that the scheme (4.3)-(4.4) admits the discrete equilibrium solution

$$(5.14) \quad \begin{aligned} \rho_K^n &= \tilde{\rho}_K, \quad \forall K \in \mathcal{M}, \quad 0 \leq n \leq N, \\ u_\sigma^n &= 0, \quad \forall \sigma \in \mathcal{E}, \quad 0 \leq n \leq N, \end{aligned}$$

with $\tilde{\rho} \in L_{\mathcal{M}}(\Omega)$ satisfying the following discrete analogue of the hydrostatic steady state (2.6):

$$(5.15) \quad (\partial_{\mathcal{E}}^{(i)} \tilde{p})_\sigma = -\tilde{\rho}_\sigma (\partial_{\mathcal{E}}^{(i)} \phi)_\sigma, \quad \forall \sigma \in \mathcal{E}_{\text{int}}^{(i)}, \quad i = 1, 2, \dots, d.$$

In the above, $\tilde{p} = \sum_{K \in \mathcal{M}} \tilde{p}_K \mathcal{X}_K \in L_{\mathcal{M}}(\Omega)$ is a discretisation of the hydrostatic pressure, i.e. $\tilde{p}_K = \wp(\tilde{\rho}_K)$, $\forall K \in \mathcal{M}$, and for each $\sigma = K|L \in \mathcal{E}_{\text{int}}^{(i)}$, $i = 1, 2, \dots, d$, the interface hydrostatic density is given by $\tilde{\rho}_\sigma = \tilde{\rho}_{KL}$, as in Lemma 3.2. Recalling the identity (3.8) and upon dividing by $\tilde{\rho}_\sigma$, the relation (5.15) further yields

$$(5.16) \quad (\partial_{\mathcal{E}}^{(i)} (h'_\gamma(\tilde{\rho}) + \phi))_\sigma = 0, \quad \forall \sigma \in \mathcal{E}_{\text{int}}^{(i)}, \quad i = 1, 2, \dots, d,$$

which serves as a discrete counter part of the identity (2.7). Note that the discrete stabilisation parameter is consistent with the steady state in the sense that $\delta \mathbf{u}^{n+1} = 0$ whenever $\rho^{n+1} = \tilde{\rho}$. The relative energy estimate (5.6) with respect to the above discrete hydrostatic steady state gives a distance between the successive numerical solutions and the stationary counterparts. Given the initial condition as the steady state solution, the estimate (5.6) is satisfied if and only if the discrete steady state remains preserved in the subsequent updates.

Theorem 5.7. *The semi-implicit scheme has the following properties.*

- (i) *Suppose $(\rho^n, \mathbf{u}^n) \in L_{\mathcal{M}}(\Omega) \times \mathbf{H}_{\mathcal{E},0}(\Omega)$, where $\rho^n > 0$, and $(\rho^{n+1}, \mathbf{u}^{n+1}) \in L_{\mathcal{M}}(\Omega) \times \mathbf{H}_{\mathcal{E},0}(\Omega)$ solves the semi-implicit scheme (4.3)-(4.4). Then $\rho_K^{n+1} = \tilde{\rho}_K$, $\forall K \in \mathcal{M}$, and $u_\sigma^{n+1} = 0$, $\forall \sigma \in \mathcal{E}^{(i)}$, $i = 1, 2, \dots, d$, if and only if*

$$(5.17) \quad \frac{1}{\varepsilon^2} \sum_{K \in \mathcal{M}} |K| \Pi_\gamma(\rho_K^{n+1} | \tilde{\rho}_K) + \sum_{\sigma \in \mathcal{E}_{\text{int}}} |D_\sigma| \frac{1}{2} \rho_{D_\sigma}^{n+1} (u_\sigma^{n+1})^2 = 0.$$

- (ii) *The semi implicit scheme is well-balanced in the following sense: given the initial data $\rho^0 = \tilde{\rho}$, $\mathbf{u}_\varepsilon^0 = \mathbf{0}$, the scheme admits the unique stationary solution $(\tilde{\rho}, \mathbf{0})$.*

Proof. The result in (i) readily follows from Theorem 5.4 on energy stability along with the fact that $\Pi_\gamma(\rho_1 | \rho_2) \geq 0$ for any $\rho_1, \rho_2 \in \mathbb{R}$ and $\Pi_\gamma(\rho_1 | \rho_2) = 0$ if and only if $\rho_1 = \rho_2$. Upon applying induction on the time-steps we obtain (ii) as a direct consequence of (i). \square

6. WEAK CONSISTENCY OF THE SCHEME

Goal of this section is to show a Lax-Wendroff-type weak consistency of the scheme (4.3)-(4.4). We consider a sequence of numerical solutions generated upon successive mesh refinements, and satisfying certain boundedness assumptions. If the sequence of solutions converges strongly to a limit, then the limit must be a weak solution of the Euler equations. Considering a bounded initial data $(\rho_0^\varepsilon, \mathbf{u}_0^\varepsilon) \in L^\infty(\Omega)^{1+d}$ and recalling the definition of a weak solution, cf. Definition 2.1, we have the following Lax-Wendroff-type consistency formulation for the semi-implicit scheme (2.1)-(2.2). In the theorem, we take the liberty to suppress ε wherever necessary for the sake of simplicity of writing.

Theorem 6.1. *Let Ω be an open bounded set of \mathbb{R}^d . Assume that $(\mathcal{T}^{(m)}, \delta t^{(m)})_{m \in \mathbb{N}}$ is a sequence of discretisations such that both $\lim_{m \rightarrow +\infty} \delta t^{(m)}$ and $\lim_{m \rightarrow +\infty} h^{(m)}$ are 0. Let $(\rho^{(m)}, \mathbf{u}^{(m)})_{m \in \mathbb{N}}$ be the corresponding sequence of discrete solutions with respect to an initial data $(\rho_0^\varepsilon, \mathbf{u}_0^\varepsilon) \in L^\infty(\Omega)^{1+d}$. We assume that $(\rho^{(m)}, \mathbf{u}^{(m)})_{m \in \mathbb{N}}$ satisfies the following.*

(i) $(\rho^{(m)}, \mathbf{u}^{(m)})_{m \in \mathbb{N}}$ is uniformly bounded in $L^\infty(Q)^{1+d}$, i.e.

$$(6.1) \quad \underline{C} < (\rho^{(m)})_K^n \leq \bar{C}, \quad \forall K \in \mathcal{M}^{(m)}, \quad 0 \leq n \leq N^{(m)}, \quad \forall m \in \mathbb{N},$$

$$(6.2) \quad |(u^{(m)})_\sigma^n| \leq C, \quad \forall \sigma \in \mathcal{E}^{(m)}, \quad 0 \leq n \leq N^{(m)}, \quad \forall m \in \mathbb{N},$$

where $\underline{C}, \bar{C}, C > 0$ are constants independent of the discretisations.

(ii) $(\rho^{(m)}, \mathbf{u}^{(m)})_{m \in \mathbb{N}}$ converges to $(\rho^\varepsilon, \mathbf{u}^\varepsilon) \in L^\infty(0, T; L^\infty(\Omega)^{1+d})$ in $L^r(Q_T)^{1+d}$ for $1 \leq r < \infty$.

We also assume that the sequence of discretisations $(\mathcal{T}^{(m)}, \delta t^{(m)})_{m \in \mathbb{N}}$ satisfies the following mesh regularity conditions:

$$(6.3) \quad \frac{\delta t^{(m)}}{\min_{K \in \mathcal{M}^{(m)}} |K|} \leq \theta, \quad \max_{K \in \mathcal{M}^{(m)}} \frac{\text{diam}(K)^2}{|K|} \leq \theta, \quad \forall m \in \mathbb{N},$$

where $\theta > 0$ is independent of the discretisations. Then, $(\rho^\varepsilon, \mathbf{u}^\varepsilon)$ satisfies the weak formulation (2.4)-(2.5).

Proof. First, we consider the limits of the discrete convection operators in (4.3)-(4.4), borrowing the results obtained in [26, 27, 32]. Since our treatment closely follows the one in the above references, we skip most of the detailed calculations and focus only on those terms arising from the stabilisation terms. We consider a smooth test function $\psi \in C_c^\infty([0, T] \times \bar{\Omega})$ and for each $m \in \mathbb{N}$, let ψ_K^n denote the average of ψ on $(t^n, t^{n+1}) \times K$ for each $n = 0, \dots, N^{(m)} - 1$, $K \in \mathcal{M}^{(m)}$. We multiply the mass update (4.3) by $\delta t |K| \psi_K^n$ and take sum over all $n = 0, \dots, N^{(m)} - 1$, $K \in \mathcal{M}^{(m)}$ to obtain

$$(6.4) \quad \sum_{n=0}^{N^{(m)}-1} \delta t \sum_{K \in \mathcal{M}^{(m)}} |K| \mathcal{C}_{\mathcal{T}^{(m)}}(\rho^{(m)}, \mathbf{u}^{(m)})_K^n \psi_K^n + R_1^{(m)} = 0,$$

where $\mathcal{C}_{\mathcal{T}^{(m)}}(\rho^{(m)}, \mathbf{u}^{(m)}) : Q_T \rightarrow \mathbb{R}$ denotes the discrete convection operator

$$(6.5) \quad \mathcal{C}_{\mathcal{T}^{(m)}}(\rho^{(m)}, \mathbf{u}^{(m)})(t, \mathbf{x}) = \sum_{n=0}^{N^{(m)}-1} \sum_{K \in \mathcal{M}^{(m)}} \mathcal{C}_{\mathcal{T}^{(m)}}(\rho^{(m)}, \mathbf{u}^{(m)})_K^n \mathcal{X}_{(t^n, t^{n+1})}(t) \mathcal{X}_K(\mathbf{x}).$$

In the above, we have denoted

$$(6.6) \quad \mathcal{C}_{\mathcal{T}^{(m)}}(\rho^{(m)}, \mathbf{u}^{(m)})_K^n = \frac{1}{\delta t}(\rho_K^{n+1} - \rho_K^n) + \frac{1}{|K|} \sum_{\substack{\sigma \in \mathcal{E}(K) \\ \sigma = K|L}} |\sigma| \rho_\sigma^{n+1} u_{\sigma,K}^n, \quad n = 0, \dots, N^{(m)} - 1, \quad K \in \mathcal{M}^{(m)}.$$

In (6.4), $R_1^{(m)}$ is the remainder term due to the velocity stabilisation given by

$$(6.7) \quad R_1^{(m)} = \sum_{n=0}^{N^{(m)}-1} \delta t^n \sum_{K \in \mathcal{M}^{(m)}} \text{diam}(K) \sum_{\sigma \in \mathcal{E}(K)} |\sigma| |\delta u_\sigma^{n+1}|.$$

Proceeding as in [27, Lemma 4.1] with the discrete convection operator (6.5)-(6.6) shows that the first term on the left hand side of (6.4) yields the weak formulation (2.4) upon taking the limit $m \rightarrow \infty$. Therefore, it remains to show that the remainder term $R_1^{(m)} \rightarrow 0$ as $m \rightarrow \infty$. To this end, we further decompose $R_1^{(m)}$ as

$$(6.8) \quad R_1^{(m)} \leq R_{1,1}^{(m)} + R_{1,2}^{(m)},$$

where

$$(6.9) \quad R_{1,1}^{(m)} = C \sum_{n=0}^{N^{(m)}-1} \delta t \sum_{K \in \mathcal{M}^{(m)}} \text{diam}(K) \sum_{\sigma \in \mathcal{E}(K)} |\sigma| \eta \delta t \frac{|\sigma|}{|D_\sigma|} |\rho_L^n - \rho_K^n|,$$

$$(6.10) \quad R_{1,2}^{(m)} = C \sum_{n=0}^{N^{(m)}-1} \delta t \sum_{K \in \mathcal{M}^{(m)}} \text{diam}(K) \sum_{\sigma \in \mathcal{E}(K)} |\sigma| \eta \delta t \frac{|\sigma|}{|D_\sigma|} |\phi_L - \phi_K|,$$

with a constant $C > 0$ depending only on ψ and \bar{C} . Applying the results on the convergence of discrete space translates, cf. [26, Lemma 4.1], we can easily see that the right hand sides of (6.9)-(6.10) tends to 0 as $m \rightarrow \infty$ under the given assumptions. Consequently, the weak consistency of the mass update (4.3) follows.

In order to prove the weak consistency of the momentum balance, we similarly start with a compactly supported smooth vector valued test function $\boldsymbol{\psi} = (\psi_i)_{i=1}^d \in C_c^\infty([0, T] \times \bar{\Omega})^d$. For each $m \in \mathbb{N}$ and $i = 1, \dots, d$, denote by $(\psi_i^{(m)})_\sigma^n$, the average of ψ_i on $(t^n, t^{n+1}) \times D_\sigma$ for $n = 0, \dots, N^{(m)} - 1$, $\sigma \in (\mathcal{E}^{(m)})_{\text{int}}^{(i)}$. We multiply the momentum update (4.4) by $(\psi_i^{(m)})_\sigma^n$ for $i = 1, \dots, d$ and take sum over all $n = 0, \dots, N^{(m)} - 1$, $\sigma \in (\mathcal{E}^{(m)})_{\text{int}}^{(i)}$. The weak consistency of the corresponding discrete convection operator and the pressure gradient can be obtained using analogous results as in [32, Theorem 4.1]. Whereas, the remainder terms due to the stabilisation terms in the momentum flux vanishes as $m \rightarrow \infty$ upon recalling similar arguments as in the case of the mass update.

Finally, the summation over all $\sigma \in \mathcal{E}_{\text{int}}^{(i)}$ and all $n \in \{0, 1, \dots, N^{(m)} - 1\}$, the source term of (4.4) yields the expression

$$(6.11) \quad T_{i,\text{source}}^{(m)} = \sum_{n=0}^{N^{(m)}-1} \delta t^n \sum_{\sigma \in \mathcal{E}_{\text{int}}^{(i)}} |D_\sigma| \rho_\sigma^n \psi_\sigma^n (\partial_{\mathcal{E}}^{(i)} \phi)_\sigma.$$

Since, $\phi \in L_{\mathcal{M}(m)}(\Omega)$ is obtained upon taking cell-averages of a smooth function, an application of [26, Lemma 3.1] and the assumptions on the sequence of discrete solutions yield,

$$(6.12) \quad T_{i,\text{source}}^{(m)} \rightarrow \iint_{Q_T} \rho \partial_{x_i} \phi \psi_i d\mathbf{x} dt, \text{ as } m \rightarrow \infty,$$

and accordingly we have the weak consistency of the momentum update (4.4). \square

7. CONSISTENCY WITH THE ANELASTIC LIMIT

With the aid of the estimates obtained in Section 5, we now proceed to obtain the asymptotic limit of the semi-implicit scheme. As a first step, we derive the following uniform estimates with respect to ε as an immediate consequence of total energy bound obtained Theorem 5.4. Consequently, we show that, for a given discretisation of the domain, the velocity stabilised semi-implicit scheme (4.3)-(4.4) converges to a velocity stabilised semi-implicit scheme for the anelastic Euler equations (2.16)-(2.17) as $\varepsilon \rightarrow 0$. Note that, in the subsequent analysis, we shall take advantage of the corresponding discrete function spaces being finite-dimensional for a fixed mesh. This feature, along with the uniform bounds, finally enables us to obtain the limit of the stiff terms as a solution of a discrete elliptic equation.

Proposition 7.1 (Global discrete energy inequality). *Let $(\rho^{n+1}, \mathbf{u}^{n+1}) \in L_{\mathcal{M}}(\Omega) \times \mathbf{H}_{\mathcal{E},0}(\Omega)$ be a solution of the semi implicit scheme (4.3)-(4.4) with respect to a well-prepared initial data $(\rho_0^\varepsilon, \mathbf{u}_0^\varepsilon) \in L^\infty(\Omega)^{1+d}$. Then $(\rho^{n+1}, \mathbf{u}^{n+1})$ satisfies the following estimate for sufficiently small $\varepsilon > 0$.*

(7.1)

$$\begin{aligned} \frac{1}{\varepsilon^2} \sum_{K \in \mathcal{M}} |K| \Pi_\gamma(\rho_K^{n+1} | \tilde{\rho}_K) + \sum_{i=1}^d \sum_{\sigma \in \mathcal{E}_{\text{int}}^{(i)}} |D_\sigma| \frac{1}{2} \rho_{D_\sigma}^{n+1} (u_\sigma^{n+1})^2 \\ + \frac{\delta t^2}{\varepsilon^4} \sum_{k=0}^n \sum_{i=1}^d \sum_{\sigma \in \mathcal{E}_{\text{int}}^{(i)}} |D_\sigma| \left(\eta - \frac{1}{\rho_{D_\sigma}^{k+1}} \right) \left((\partial_{\mathcal{E}}^{(i)} p^{k+1})_\sigma + \rho_\sigma^{k+1} (\partial_{\mathcal{E}}^{(i)} \phi)_\sigma \right)^2 \leq C, \end{aligned}$$

where $C > 0$ is a constant independent of ε .

Proof. Upon multiplying (5.12) by δt and taking sum over time-steps from 0 to $n - 1$ we obtain that, any solution $(\rho^{n+1}, \mathbf{u}^{n+1}) \in L_{\mathcal{M}}(\Omega) \times \mathbf{H}_{\mathcal{E},0}(\Omega)$ of (4.3)-(4.4) satisfies

$$\begin{aligned} \frac{1}{\varepsilon^2} \sum_{K \in \mathcal{M}} |K| \Pi_\gamma(\rho_K^{n+1} | \tilde{\rho}_K) + \sum_{i=1}^d \sum_{\sigma \in \mathcal{E}_{\text{int}}^{(i)}} |D_\sigma| \frac{1}{2} \rho_{D_\sigma}^{n+1} (u_\sigma^{n+1})^2 \\ + \frac{\delta t^2}{\varepsilon^4} \sum_{k=0}^n \sum_{i=1}^d \sum_{\sigma \in \mathcal{E}_{\text{int}}^{(i)}} |D_\sigma| \left(\eta - \frac{1}{\rho_{D_\sigma}^{k+1}} \right) \left((\partial_{\mathcal{E}}^{(i)} p^{k+1})_\sigma + \rho_\sigma^{k+1} (\partial_{\mathcal{E}}^{(i)} \phi)_\sigma \right)^2 \\ \leq \frac{1}{\varepsilon^2} \sum_{K \in \mathcal{M}} |K| \Pi_\gamma(\rho_K^0 | \tilde{\rho}_K) + \sum_{\sigma \in \mathcal{E}_{\text{int}}} |D_\sigma| \frac{1}{2} \rho_{D_\sigma}^0 (u_\sigma^0)^2. \end{aligned} \quad (7.2)$$

The uniform bound of the right hand side of (7.2) with respect to ε follows from Lemma 4.3. \square

Carrying out a treatment analogous to the one performed for the continuous case in Section 2, we obtain the following estimates for the scheme (4.3)-(4.4) as $\varepsilon \rightarrow 0$.

Lemma 7.2. *Let $\mathcal{T} = (\mathcal{M}, \mathcal{E})$ be a fixed primal-dual mesh pair that gives a MAC grid discretisation of $\bar{\Omega}$ and let $\delta t > 0$ be such that $\{0 = t^0 < t^1 < \dots < t^N = T\}$ is a discretisation of the time domain $[0, T]$ with $\delta t = t^n - t^{n-1}$ for $1 \leq n \leq N$. For each $\varepsilon > 0$, let us denote by $(\rho^\varepsilon, \mathbf{u}^\varepsilon) \in L^\infty(0, T; L_{\mathcal{M}}(\Omega) \times \mathbf{H}_{\mathcal{E}, 0}(\Omega))$ the approximate solutions to the semi-implicit scheme (4.3)-(4.4) with respect to a well-prepared initial data $(\rho_0^\varepsilon, \mathbf{u}_0^\varepsilon) \in L^\infty(\Omega)^{1+d}$. Then we have the following.*

- (i) $\rho^\varepsilon \rightarrow \tilde{\rho}$ as $\varepsilon \rightarrow 0$ in $L^\infty(0, T; L^r(\Omega))$, for any $r \in (1, \min\{2, \gamma\}]$, where $\tilde{\rho} = \sum_{K \in \mathcal{M}} \tilde{\rho}_K \mathcal{X}_K \in L_{\mathcal{M}}(\Omega)$ denotes the discrete approximation of the hydrostatic density.
- (ii) The sequence of approximate solutions for the velocity component $\{\mathbf{u}^\varepsilon\}_{\varepsilon > 0} \subset \mathbf{H}_{\mathcal{E}, 0}(\Omega)$ is uniformly bounded with respect to ε , i.e. for all $\varepsilon > 0$ sufficiently small, we have

$$(7.3) \quad \|\mathbf{u}^\varepsilon\|_{L^\infty(0, T; L^2(\Omega)^d)} \leq C,$$

where $C > 0$ is a constant independent of ε .

Proof. Let $\underline{\rho} > 0$, $\bar{\rho} > 0$ be such that

$$(7.4) \quad \underline{\rho} := \inf_{x \in \Omega} \tilde{\rho}(x), \quad \bar{\rho} := \sup_{x \in \Omega} \tilde{\rho}(x).$$

From (7.1) and the fact that $\Pi_\gamma(a|b) > 0$ for any $a, b \in \mathbb{R}$, we obtain that a discrete solution $\rho^\varepsilon \in L_{\mathcal{M}}(\Omega)$ of (4.3)-(4.4) satisfies

$$(7.5) \quad |K| \Pi_\gamma((\rho^\varepsilon)_K^{n+1} | \tilde{\rho}_K) \leq C\varepsilon^2, \quad \forall K \in \mathcal{M}, \quad n = 0, \dots, N-1,$$

where $C > 0$ is a constant independent of ε . Analogously as in the the proof of [1, Lemma 6.2], for any $\gamma > 2$, we get

$$(7.6) \quad |K| |(\rho^\varepsilon)_K^{n+1} - \tilde{\rho}_K|^2 \leq C\varepsilon^2, \quad \forall K \in \mathcal{M}, \quad n = 0, \dots, N-1,$$

and for any $\gamma \in (1, 2)$, and each $n \in \{0, 1, \dots, N-1\}$, we have

$$(7.7) \quad |K| |(\rho^\varepsilon)_K^{n+1} - \tilde{\rho}_K|^2 \leq C\varepsilon^2, \quad \forall K \in \mathcal{M}_{\text{ess}}^\varepsilon,$$

$$(7.8) \quad |K| |(\rho^\varepsilon)_K^{n+1} - \tilde{\rho}_K|^\gamma \leq C\varepsilon^2, \quad \forall K \in \mathcal{M}_{\text{res}}^\varepsilon.$$

Here, the essential and residual parts are defined by $\mathcal{M}_{\text{ess}}^\varepsilon := \{K \in \mathcal{M} : (\rho^\varepsilon)_K^{n+1} < 2\bar{\rho}\}$ and $\mathcal{M}_{\text{res}}^\varepsilon := \{K \in \mathcal{M} : (\rho^\varepsilon)_K^{n+1} \geq 2\bar{\rho}\}$. In all the estimates (7.6)-(7.8) above, $C > 0$ denotes a constant independent of ε which in turn yields the convergence of ρ^ε as stated in (i). From the estimates (7.6)-(7.8) we further obtain that for a fixed space-time discretisation, $(\rho^\varepsilon)_K^n \rightarrow \tilde{\rho}_K$ as $\varepsilon \rightarrow 0$ for each $K \in \mathcal{M}$ and $1 \leq n \leq N$. Subsequently, for $\varepsilon > 0$, sufficiently small, we have

$$(7.9) \quad 0 < \underline{\rho} \leq (\rho^\varepsilon)_K^n \leq \bar{\rho}, \quad \forall K \in \mathcal{M}, \quad 1 \leq n \leq N.$$

The estimate (7.3) in (ii) readily follows from the kinetic energy component of the total energy estimate (7.1) and the uniform lower bound of $\{\rho^\varepsilon\}_{\varepsilon > 0}$ obtained in (7.9) for sufficiently small values of ε . \square

In order to study the convergence of the stiff terms as the Mach/Froude numbers vanish, we first obtain the following discrete L^2 -control that comes as a consequence of the uniform bound obtained in Proposition 7.1.

Lemma 7.3. *Let $\mathcal{T} = (\mathcal{M}, \mathcal{E})$ and $\delta t > 0$ be as in Lemma 7.2. Let $\varepsilon > 0$ be fixed and let $(\rho^n, \mathbf{u}^n)_{1 \leq n \leq N} \subset L_{\mathcal{M}}(\Omega) \times \mathbf{H}_{\mathcal{E}, 0}(\Omega)$ be a solution of the scheme (4.3)-(4.4) with respect to a well-prepared initial data $(\rho_0^\varepsilon, \mathbf{u}_0^\varepsilon) \in L^\infty(\Omega)^{1+d}$. Then there exists a constant $C > 0$, independent of ε ,*

such that for each $1 \leq n \leq N$,

$$(7.10) \quad \frac{1}{\varepsilon^4} \sum_{i=1}^d \sum_{\sigma \in \mathcal{E}_{\text{int}}^{(i)}} |D_\sigma| \left((\partial_\mathcal{E}^{(i)} p^n)_\sigma + \rho_\sigma^n (\partial_\mathcal{E}^{(i)} \phi)_\sigma \right)^2 < C,$$

which further yields,

$$(7.11) \quad \frac{1}{\varepsilon^4} \sum_{i=1}^d \sum_{\sigma \in \mathcal{E}_{\text{int}}^{(i)}} |D_\sigma| \left((\partial_\mathcal{E}^{(i)} (h'_\gamma(\rho^n) + \phi))_\sigma \right)^2 < C.$$

Proof. From the energy estimate (7.1) we note that for $\varepsilon > 0$, small enough, and for each $1 \leq n \leq N$, the following holds:

$$(7.12) \quad \frac{1}{\varepsilon^4} \sum_{i=1}^d \sum_{\sigma \in \mathcal{E}_{\text{int}}^{(i)}} |D_\sigma| \left(\eta - \frac{1}{\rho_{D_\sigma}^n} \right) \left((\partial_\mathcal{E}^{(i)} p^n)_\sigma + \rho_\sigma^n (\partial_\mathcal{E}^{(i)} \phi)_\sigma \right)^2 \leq C,$$

where the constant $C > 0$ is independent of ε , but depends on $\underline{\rho}, \bar{\rho}$, the domain Q_T , and the fixed discretisation $(\delta t, \mathcal{T})$. The choice of the constant η in accordance with the inequality (5.13), imposed by the time-step restriction, yields (7.10). An application of the identity (3.8) related to the choice ρ_σ and the uniform bounds (7.9) on ρ^ε yield (7.11) from (7.10). \square

We have the following corollary on the limit of the stiff terms as an immediate consequence of the uniform estimate (7.10).

Corollary 7.4. *For each $n = 1, \dots, N$, there exists $\theta^n \in \mathbf{H}_{\mathcal{E},0}(\Omega)$ such that $\{\frac{1}{\varepsilon^2}(\nabla_\mathcal{E} p^n + \rho^n \nabla_\mathcal{E} \phi)\}_{\varepsilon>0}$ weakly converges to θ^n in $L^2(\Omega)^d$.*

Proof. From Lemma 7.3 we note that $\{\frac{1}{\varepsilon^2}(\nabla_\mathcal{E} p^n + \rho^n \nabla_\mathcal{E} \phi)\}_{\varepsilon>0} \subset \mathbf{H}_{\mathcal{E},0}(\Omega)$ is uniformly bounded in $L^2(\Omega)^d$ for each $n = 1, \dots, N$ and hence admits a weak limit $\theta^n \in L^2(\Omega)^d$ as $\varepsilon \rightarrow 0$. Since $\mathbf{H}_{\mathcal{E},0}(\Omega)$ is weakly closed in $L^2(\Omega)^d$ as it is a finite dimensional subspace of $L^2(\Omega)^d$, we conclude that $\theta^n \in \mathbf{H}_{\mathcal{E},0}(\Omega)$ for each $n = 1, \dots, N$. \square

The following lemma provides a description of the weak limit θ^n of the stiff terms; cf. Corollary 2.8 for the analogous result in the continuous case.

Lemma 7.5. *For each $n = 1, \dots, N$, there exists $\pi^n \in L_{\mathcal{M}}(\Omega)$ such that*

$$(7.13) \quad \theta_\sigma^n = \tilde{\rho}_\sigma (\partial_\mathcal{E}^{(i)} \pi^n)_\sigma, \quad \sigma \in \mathcal{E}_{\text{int}}^{(i)}, \quad i = 1, 2, \dots, d.$$

Proof. First, we claim that the following identity holds for any $\psi \in \mathbf{H}_{\mathcal{E},0}(\Omega)$ with $\text{div}_{\mathcal{M}}(\tilde{\rho}\psi) = 0$:

$$(7.14) \quad \sum_{i=1}^d \sum_{\sigma \in \mathcal{E}_{\text{int}}^{(i)}} |D_\sigma| \theta_\sigma^n \psi_\sigma = 0.$$

Note that, for any $\psi \in \mathbf{H}_{\mathcal{E},0}(\Omega)$ satisfying $\operatorname{div}_{\mathcal{M}}(\tilde{\rho}\psi) = 0$, we have

$$\begin{aligned}
& \frac{1}{\varepsilon^2} \sum_{i=1}^d \sum_{\sigma \in \mathcal{E}_{\text{int}}^{(i)}} |D_{\sigma}| \left((\partial_{\mathcal{E}}^{(i)} p^n)_{\sigma} + \rho_{\sigma}^n (\partial_{\mathcal{E}}^{(i)} \phi)_{\sigma} \right) \psi_{\sigma} \\
&= \frac{1}{\varepsilon^2} \sum_{i=1}^d \sum_{\sigma \in \mathcal{E}_{\text{int}}^{(i)}} |D_{\sigma}| \rho_{\sigma}^n \left((\partial_{\mathcal{E}}^{(i)} (h'_{\gamma}(\rho^n + \phi)))_{\sigma} \right) \psi_{\sigma} \\
(7.15) \quad &= \frac{1}{\varepsilon^2} \sum_{i=1}^d \sum_{\sigma \in \mathcal{E}_{\text{int}}^{(i)}} |D_{\sigma}| (\rho_{\sigma}^n - \tilde{\rho}_{\sigma}) \left((\partial_{\mathcal{E}}^{(i)} (h'_{\gamma}(\rho^n + \phi)))_{\sigma} \right) \psi_{\sigma} \\
&\quad + \frac{1}{\varepsilon^2} \sum_{i=1}^d \sum_{\sigma \in \mathcal{E}_{\text{int}}^{(i)}} |D_{\sigma}| \tilde{\rho}_{\sigma} \left((\partial_{\mathcal{E}}^{(i)} (h'_{\gamma}(\rho^n + \phi)))_{\sigma} \right) \psi_{\sigma}.
\end{aligned}$$

Applying the Cauchy-Schwarz inequality, the first term on the right hand side of (7.15) yields

$$\begin{aligned}
(7.16) \quad & \frac{1}{\varepsilon^2} \left| \sum_{i=1}^d \sum_{\sigma \in \mathcal{E}_{\text{int}}^{(i)}} |D_{\sigma}| (\rho_{\sigma}^n - \tilde{\rho}_{\sigma}) \left((\partial_{\mathcal{E}}^{(i)} (h'_{\gamma}(\rho^n + \phi)))_{\sigma} \right) \psi_{\sigma} \right| \\
& \leq C_{\psi} \left(\sum_{i=1}^d \sum_{\sigma \in \mathcal{E}_{\text{int}}^{(i)}} |D_{\sigma}| |\rho_{\sigma}^n - \tilde{\rho}_{\sigma}|^2 \right)^{\frac{1}{2}} \left(\frac{1}{\varepsilon^4} \sum_{i=1}^d \sum_{\sigma \in \mathcal{E}_{\text{int}}^{(i)}} |D_{\sigma}| |(\partial_{\mathcal{E}}^{(i)} (h'_{\gamma}(\rho^n + \phi)))_{\sigma}|^2 \right)^{\frac{1}{2}},
\end{aligned}$$

where $C_{\psi} > 0$ is a constant that depends only on ψ . The uniform bound (7.11) and the convergence of $\rho^n \in L_{\mathcal{M}}(\Omega)$, detailed in Lemma 7.2, along with a finite dimensional argument shows that the right hand side of (7.16) goes to 0 as $\varepsilon \rightarrow 0$. The second term on the right hand side of (7.15) vanishes after using the div-grad duality (3.12) and noting that $\operatorname{div}_{\mathcal{M}}(\tilde{\rho}\psi) = 0$. Therefore, the claim (7.14) is proved upon passing to the limit $\varepsilon \rightarrow 0$ in (7.16), using Corollary 7.4.

Next, we introduce a function $\pi^n \in L_{\mathcal{M}}(\Omega)$, for each $n = 1, \dots, N$, via the solution of the discrete Neumann elliptic boundary value problem

$$\begin{aligned}
(7.17) \quad & \Delta_{\mathcal{M}} \pi^n = \operatorname{div}_{\mathcal{M}} \left(\frac{1}{\tilde{\rho}} \boldsymbol{\theta}^n \right), \\
& (\nabla_{\mathcal{E}} \pi^n)_{\sigma} = 0, \quad \forall \sigma \in \mathcal{E}_{\text{ext}}^{(i)}, \quad i = 1, \dots, d.
\end{aligned}$$

The above problem gives rise to the following $\#\mathcal{M} \times \#\mathcal{M}$ system of linear equations for the unknowns $(\pi_K^n)_{K \in \mathcal{M}}$:

$$(7.18) \quad \sum_{\substack{\sigma \in \mathcal{E}(K) \\ \sigma = K|L}} \frac{|\sigma|^2}{|D_{\sigma}|} (\pi_L^n - \pi_K^n) = |K| \left(\operatorname{div}_{\mathcal{M}} \left(\frac{1}{\tilde{\rho}} \boldsymbol{\theta}^n \right) \right)_K, \quad \forall K \in \mathcal{M}.$$

Note that the right hand side of (7.18) satisfies the compatibility condition

$$(7.19) \quad \sum_{K \in \mathcal{M}} |K| \left(\operatorname{div}_{\mathcal{M}} \left(\frac{1}{\tilde{\rho}} \boldsymbol{\theta}^n \right) \right)_K = \sum_{K \in \mathcal{M}} |K| \sum_{\sigma \in \mathcal{E}(K)} |\sigma| \frac{1}{\tilde{\rho}_{\sigma}} \boldsymbol{\theta}_{\sigma,K}^n = 0.$$

Hence, the system of linear equations (7.18) admits a solution $(\pi_K^n)_{K \in \mathcal{M}} \equiv \pi^n \in L_{\mathcal{M}}(\Omega)$, unique upto an additive constant; see [19, Lemma 3.6]. Finally, we define $\boldsymbol{\xi} = (\xi^{(i)})_{i=1}^d \in \mathbf{H}_{\mathcal{E},0}(\Omega)$, where

$\xi^{(i)} = \sum_{\sigma \in \mathcal{E}_{\text{int}}^{(i)}} \xi_{\sigma} \mathcal{X}_{D_{\sigma}}$, $i = 1, \dots, d$, is given by

$$(7.20) \quad \xi_{\sigma} := (\partial_{\mathcal{E}}^{(i)} \pi^n)_{\sigma} - \frac{1}{\tilde{\rho}_{\sigma}} \theta_{\sigma}^n.$$

Since π^n solves (7.17), we notice that $\text{div}_{\mathcal{M}} \boldsymbol{\xi} = 0$ and the identity (7.14) further implies that

$$(7.21) \quad \sum_{i=1}^d \sum_{\sigma \in \mathcal{E}_{\text{int}}^{(i)}} |D_{\sigma}| \theta_{\sigma}^n \frac{\xi_{\sigma}}{\tilde{\rho}_{\sigma}} = 0.$$

Now, for each $\sigma \in \mathcal{E}_{\text{int}}^{(i)}$, $i = 1, \dots, d$, replacing θ_{σ}^n using (7.20) in (7.21), we have

$$(7.22) \quad \sum_{i=1}^d \sum_{\sigma \in \mathcal{E}_{\text{int}}^{(i)}} |D_{\sigma}| ((\partial_{\mathcal{E}}^{(i)} \pi^n)_{\sigma} - \xi_{\sigma}) \xi_{\sigma} = 0.$$

An application of the div-grad duality (3.13) and the fact that $\text{div}_{\mathcal{M}} \boldsymbol{\xi} = 0$, the above expression yields

$$(7.23) \quad \sum_{i=1}^d \sum_{\sigma \in \mathcal{E}_{\text{int}}^{(i)}} |D_{\sigma}| |\xi_{\sigma}|^2 = 0,$$

and hence we have (7.13). \square

Based on these convergences and the uniform boundedness obtained in Lemmas 7.2 and 7.5, we deduce the following theorem, where we show that the velocity stabilised semi-implicit scheme (4.3)-(4.4) converges to a velocity stabilised semi-implicit scheme for the anelastic Euler system as $\varepsilon \rightarrow 0$.

Theorem 7.6. *Let $(\varepsilon^{(k)})_{k \in \mathbb{N}}$ be a sequence of positive numbers such that $\varepsilon^{(k)} \rightarrow 0$ as $k \rightarrow \infty$. Let $\{(\rho^{(k)}, \mathbf{u}^{(k)})\}_{k \in \mathbb{N}}$ be the corresponding sequence of numerical solutions obtained from the scheme (4.3)-(4.4) with respect to a sequence of well-prepared initial data $\{(\rho_0^{(k)}, \mathbf{u}_0^{(k)})\}_{k \in \mathbb{N}} \subset L^{\infty}(\Omega)^{1+d}$. Then $\{\rho^{(k)}\}_{k \in \mathbb{N}}$ converges to $\tilde{\rho} \in L_{\mathcal{M}}(\Omega)$ in $L^{\infty}(0, T; L^r(\Omega))$ for any $r \in (1, \min\{2, \gamma\}]$ and so in any discrete norm on $L_{\mathcal{M}}(\Omega)$. Furthermore, there exists $(\pi, \mathbf{U}) \in L^{\infty}(0, T; L_{\mathcal{M}}(\Omega) \times \mathbf{H}_{\mathcal{E}, 0}(\Omega))$ such that $\{\mathbf{u}^{(k)}\}_{k \in \mathbb{N}}$ converges to $\mathbf{U} \in L^{\infty}(0, T; \mathbf{H}_{\mathcal{E}, 0}(\Omega))$ in any discrete norm as $k \rightarrow \infty$ and the piecewise constant function $\{(\pi^n, \mathbf{U}^n)\}_{1 \leq n \leq N} \subset L_{\mathcal{M}}(\Omega) \times \mathbf{H}_{\mathcal{E}, 0}(\Omega)$ is defined as follows.*

Given $(\pi^n, \mathbf{U}^n) \in L_{\mathcal{M}}(\Omega) \times \mathbf{H}_{\mathcal{E}, 0}(\Omega)$ at time t^n , $(\pi^{n+1}, \mathbf{U}^{n+1}) \in L_{\mathcal{M}}(\Omega) \times \mathbf{H}_{\mathcal{E}, 0}(\Omega)$ solves the semi-implicit scheme

$$(7.24) \quad (\text{div}_{\mathcal{M}}(\tilde{\rho}(\mathbf{U}^n - \delta \mathbf{U}^{n+1})))_K = 0, \quad \forall K \in \mathcal{M},$$

$$(7.25) \quad \frac{1}{\delta t} \tilde{\rho}_{D_{\sigma}} (U_{\sigma}^{n+1} - U_{\sigma}^n) + \frac{1}{|D_{\sigma}|} \sum_{\epsilon \in \mathcal{E}(D_{\sigma})} F_{\epsilon, \sigma}(\tilde{\rho}, \mathbf{U}^n - \delta \mathbf{U}^{n+1}) U_{\epsilon, \text{up}}^n + \tilde{\rho}_{\sigma} (\partial_{\mathcal{E}}^{(i)} \pi^{n+1})_{\sigma} = 0, \quad 1 \leq i \leq d, \quad \forall \sigma \in \mathcal{E}_{\text{int}}^{(i)},$$

with the correction term $(\delta \mathbf{U}^{n+1})_{\sigma} = \eta \delta t (\partial_{\mathcal{E}}^{(i)} \pi^{n+1})_{\sigma}$, $\eta > \frac{1}{\tilde{\rho}_{D_{\sigma}}}$ for $\sigma \in \mathcal{E}_{\text{int}}^{(i)}$, $i = 1, 2, \dots, d$.

8. NUMERICAL CASE STUDIES

In this section, we present the results of several numerical tests performed with the proposed scheme (4.3)-(4.4). The stability analysis performed in Section 5, cf. Theorem 5.4, requires that the time-steps δt are to be chosen according to the condition

$$(8.1) \quad \frac{\delta t}{|D_\sigma|} \sum_{\epsilon \in \tilde{\mathcal{E}}(D_\sigma)} \frac{F_{\epsilon,\sigma}(\rho^{n+1}, \mathbf{u}^n)^-}{\rho_{D_\sigma}^{n+1}} \leq \frac{1}{2}, \quad \forall \sigma \in \mathcal{E}^{(i)}, \quad i = 1, \dots, d.$$

Since the above stability condition is implicit, carrying out the analogous calculations as done in [13, 15, 16], we obtain the following sufficient condition on the time-step which is easier to implement in practice. Nonetheless, the sufficient condition is still implicit and we impose it in an explicit fashion.

Proposition 8.1. *Suppose $\delta t > 0$ be such that for each $\sigma \in \mathcal{E}^{(i)}$, $i \in \{1, \dots, d\}$, $\sigma = K|L$, the following holds:*

$$(8.2) \quad \delta t \max \left\{ \frac{|\partial K|}{|K|}, \frac{|\partial L|}{|L|} \right\} \left(|u_\sigma^n| + \frac{\sqrt{\eta}}{\varepsilon} \left| (p_L^{n+1} - p_K^{n+1}) + \rho_\sigma^{n+1} (\phi_L - \phi_K) \right|^{\frac{1}{2}} \right) \leq \min \left\{ 1, \frac{1}{3} \mu_{K,L}^{n,n+1} \right\},$$

where $|\partial K| = \sum_{\sigma \in \mathcal{E}(K)} |\sigma|$ and $\mu_{K,L}^{n,n+1} = \frac{\min\{\rho_K^n, \rho_L^n\}}{\max\{\rho_K^{n+1}, \rho_L^{n+1}\}}$. Then δt satisfies the inequality (8.1).

Proof. We omit the proof and refer to [13, Proposition 3.2] for calculations done in the case of an explicit scheme; see also [1] for an analogous result derived for a velocity stabilised semi-implicit scheme applied to the barotropic Euler system without source terms. \square

Remark 8.2. The numerical implementation of the scheme (4.3)-(4.4) is done as follows. First, the mass conservation equation (4.3) is solved to get the updated density ρ^{n+1} . A Newton iteration has to be performed due to the presence of nonlinear stabilisation terms. In our experiments, we note that the iterations converge in 2-3 steps. Once ρ^{n+1} is calculated, the momentum update (4.4) is evaluated explicitly to get the velocity \mathbf{u}^{n+1} .

8.1. Well-Balancing Test. In this test case we show that a hydrostatic steady state is exactly preserved by the scheme uniformly with respect to ε . We consider the following one-dimensional (1D) steady state initial data:

$$\rho(0, x) = \tilde{\rho}(x) = \left(1 - \frac{\gamma - 1}{\gamma} \phi(x) \right)^{\frac{1}{\gamma-1}}, \quad u(0, x) = 0,$$

in the domain $[0, 1]$ under three gravitational potentials defined by the choices $\phi(x) = x, \frac{1}{2}x^2, \sin(2\pi x)$. The value of the adiabatic constant is $\gamma = 1.4$. The domain is discretised into 100 grid points and the L^1 -errors of the density and momentum with respect to the above exact solution are calculated until a final time $T = 2$. In Table 1 we present the errors for different values of ε corresponding to both the compressible and stiff anelastic regimes. We observe that the velocity stabilised semi-implicit scheme approximates the steady state with high precision, irrespective of the choices of ϕ and irrespective of the asymptotic regime.

$\phi(x)$	ε	L^1 -error in ρ	L^1 -error in ρu
x	10^{-1}	5.7732E-17	1.0495E-13
	10^{-2}	7.0777E-17	3.8677E-13
	10^{-3}	6.8001E-17	1.0013E-13
$\frac{1}{2}x^2$	10^{-1}	3.7192E-17	1.0722E-13
	10^{-2}	3.9968E-17	1.7715E-13
	10^{-3}	3.9413E-17	4.7424E-14
$\sin(2\pi x)$	10^{-1}	2.0983E-16	2.4883E-13
	10^{-2}	2.2260E-16	4.3341E-13
	10^{-3}	2.1122E-16	1.6502E-13

TABLE 1. L^1 -errors with respect to a 1D hydrostatic equilibrium.

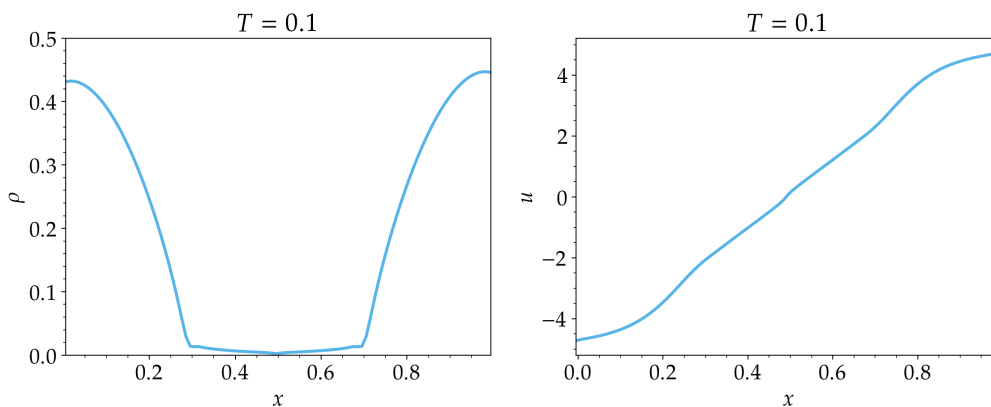
8.2. Strong Rarefaction. This case study is to showcase the scheme's capability of preserving the positivity of density under a strong rarefaction. In that order we solve the following extreme Riemann problem from [41]. The initial density is given by the hydrostatic equilibrium

$$\rho(0, x, y) = \tilde{\rho}(x, y) = \left(1 - \frac{\gamma - 1}{\gamma} \phi(x, y)\right)^{\frac{1}{\gamma-1}},$$

under the gravitational potential $\phi(x, y) = \frac{1}{2}((x - 0.5)^2 + (y - 0.5)^2)$. The initial velocity is given by

$$(8.3) \quad u(0, x, y) = \begin{cases} -5, & \text{if } x \leq 0.5, \\ 5, & \text{if } x > 0.5, \end{cases} \quad v(0, x, y) = 0.$$

The computational domain $[0, 1] \times [0, 1]$ is discretised into 100×100 mesh points. Extrapolation boundary conditions are applied on all sides of the domain. The adiabatic constant is chosen as $\gamma = 2$ and the simulations are run till the time $T = 0.1$. Due to the symmetry, we plot only the cross-sections of the density and velocity profiles along the x -direction in Figure 1. The results clearly indicate the formation of vacuum in the middle of the domain and the scheme's excellent capability to maintain the positivity of density.

FIGURE 1. Cross-sections of density and velocity profiles at time $T = 0.1$ for the strong rarefaction problem.

8.3. Sod Problem with Gravitational Potential. This case study is the classical 1D Sod shock tube problem. Our goal is to demonstrate the scheme's capability of resolving shock discontinuities in the compressible regime. The initial conditions are given by

$$(8.4) \quad \rho(0, x) = \begin{cases} 1, & \text{if } x < 0.5, \\ 0.125, & \text{if } x \geq 0.5, \end{cases} \quad u(0, x) = 0.$$

The computational domain is $[0, 1]$ and a linear gravitational potential $\phi(x) = x$ is taken. The domain is discretised with 200 grid points. Solid wall boundary conditions are applied on both the ends. In order to simulate the compressible regime, we choose $\varepsilon = 1$ and the adiabatic constant is taken as $\gamma = 1.4$. The simulations are run till the time $T = 0.2$. We compare the computed density and velocity profiles to a reference solution obtained using a classical explicit Rusanov scheme on a fine mesh of 2000 points. The results are depicted in Figure 2 which clearly shows a good agreement between the two solutions. It can be noted that the scheme well captures the shock front propagating towards the right followed by an expansion and that it emulates the speed of the shock propagation correctly.

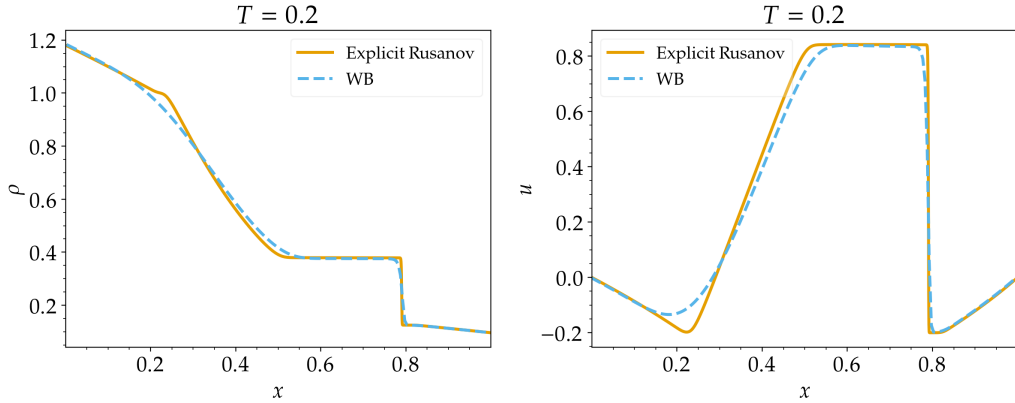


FIGURE 2. Density and velocity profiles for the Sod problem at time $T = 0.2$.

8.4. 1D Perturbation of Hydrostatic Steady State. We test the performance of the proposed well-balanced AP scheme in simulating the perturbation of a steady state against a non well-balanced scheme for a range of values of ε from the non-stiff to stiff regimes. The setup consists of adding a small perturbation to a hydrostatic density profile and setting the velocities to zero. The computational domain is $[0, 1]$ and the initial condition reads

$$(8.5) \quad \rho(0, x) = \left(1 - \frac{\gamma - 1}{\gamma} \phi(x)\right)^{\frac{1}{\gamma-1}} + \zeta e^{-100(x-0.5)^2},$$

$$(8.6) \quad u(0, x) = 0.$$

We choose the gravitational potential function $\phi(x) = x$, the gas constant $\gamma = 1.4$, and the final time $T = 0.25$. The domain is discretised using 100 grid points. The boundary conditions are implemented by interpolating the steady state values for all the variables in the ghost cells.

In Figure 3 we plot the density perturbations obtained using $\varepsilon = 1$ for the well-balanced and a non well-balanced Rusanov scheme. The amplitudes of the perturbation are taken as $\zeta = 10^{-3}$ and 10^{-5} . Figure 3(A) indicates that when $\zeta = 10^{-3}$, both the schemes diminish the perturbations even though the well-balanced scheme shows a superior performance. However, when the steady state is

approached, i.e. when $\zeta = 10^{-5}$, the non well-balanced scheme fails to capture the perturbations as evident from Figures 3(B) and 3(C).

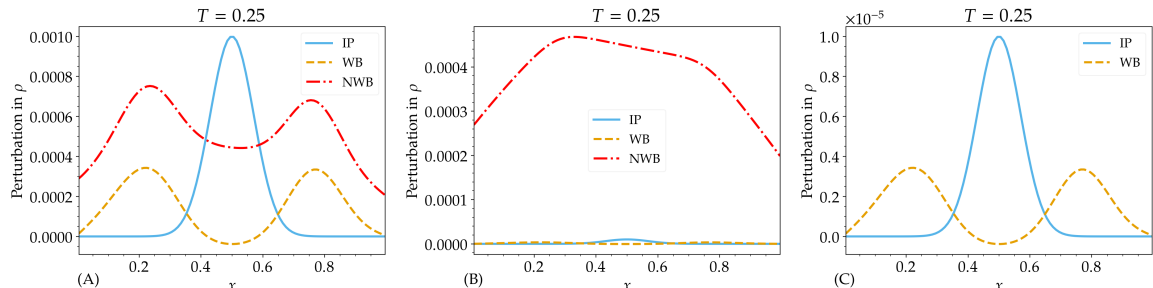


FIGURE 3. Comparison of the perturbations in density at time $T = 0.25$ for $\varepsilon = 1$. (A) $\zeta = 10^{-3}$ and (B) $\zeta = 10^{-5}$. (C) Zoom of the plot in (B) for the initial perturbation and the well-balanced scheme.

Next, we consider the stiff regime and set $\varepsilon = 0.1, 0.01$ and 0.001 . The amplitude of the perturbation in (8.5) is taken as $\zeta = \varepsilon^2$ to simulate a well-prepared initial data. We notice a blow-up of the density computed by the Rusanov scheme when $\varepsilon = 0.1$, and for smaller values of ε the Rusanov code even crashes. However, in all the cases, the well-balanced AP scheme is able to produce the correct solution even on a coarse mesh of 100 points. The results obtained are plotted in Figures 4(A)-4(C).

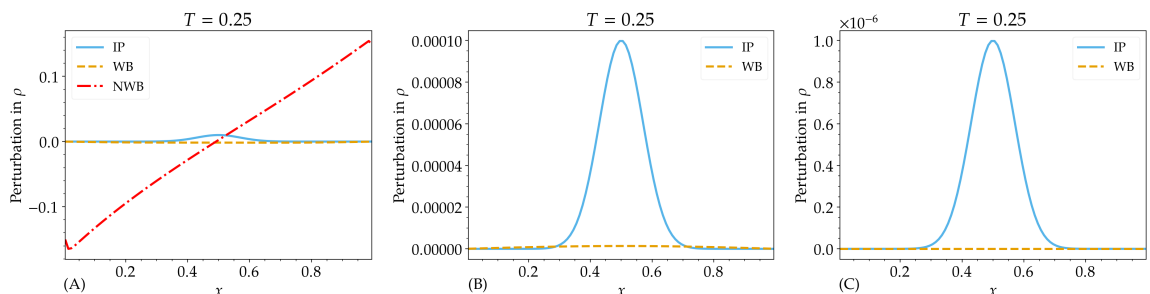


FIGURE 4. Comparison of the perturbations in density at time $T = 0.25$. (A) $\varepsilon = 0.1$, (B) $\varepsilon = 0.01$ and (C) $\varepsilon = 0.001$. The amplitude of the perturbation is $\zeta = \varepsilon^2$. The non well-balanced scheme crashes beyond $\varepsilon = 0.1$.

8.5. 2D Perturbation of Hydrostatic Steady State. We consider the following two-dimensional (2D) test case where we add a small perturbation to the hydrostatic density. The computational domain is $[0, 1] \times [0, 1]$ and the initial conditions are given by

$$\rho(0, x, y) = \left(1 - \frac{\gamma - 1}{\gamma} \phi(x, y)\right)^{\frac{1}{\gamma - 1}} + \zeta e^{-100[(x-0.3)^2 + (y-0.3)^2]},$$

$$(u, v)(0, x, y) = (0, 0).$$

We choose the gravitational potential function $\phi(x, y) = x + y$ and the adiabatic constant $\gamma = 1.4$. Note that ϕ is not aligned with the coordinate directions. The domain is discretised with 50×50 grid points and transmissive boundary conditions are taken on all sides of the domain. We simulate

the flow using the well-balanced AP scheme and a non well-balanced explicit Rusanov scheme and assess the performance of the two.

First, we consider the non-stiff ($\varepsilon = 1$) case and set the amplitude of the perturbation to $\zeta = 10^{-1}$ and 10^{-3} . The final time of the run is taken as $T = 0.05$. In Figures 5 and 6 we plot the density perturbations obtained for the two values of ζ . The results clearly indicate the superior performance of the well-balanced scheme over its non well-balanced counterpart which produces distortions near the boundary. The circular structure of the perturbations are well resolved by the well-balanced scheme despite the gravitational field being non-aligned with the coordinate axes.

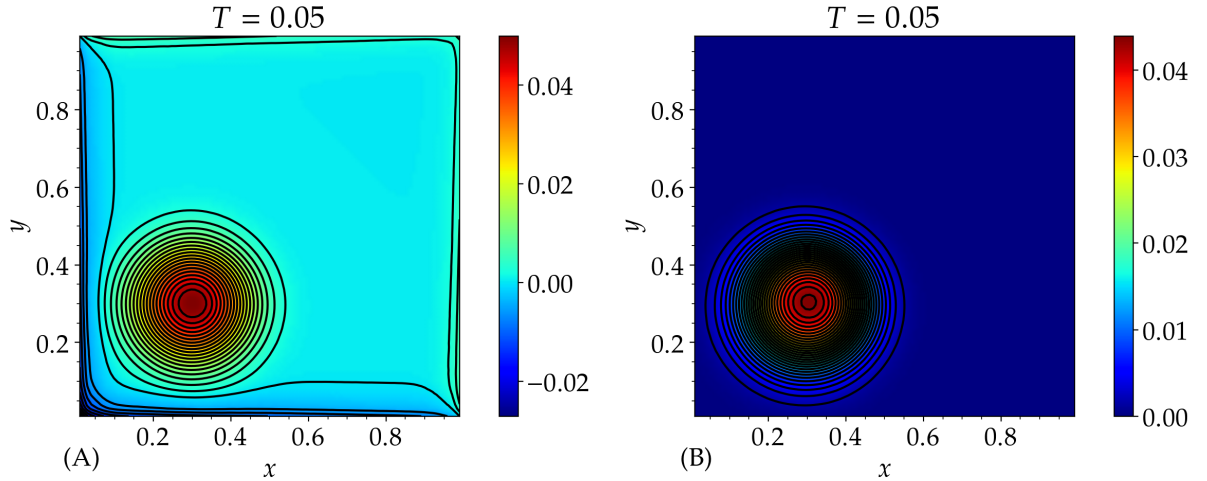


FIGURE 5. Pseudo-colour plots and contours of the density perturbations obtained by (A) the non well-balanced explicit scheme and (B) the well-balanced scheme at time $T = 0.05$ with $\varepsilon = 1$ and $\zeta = 10^{-1}$.

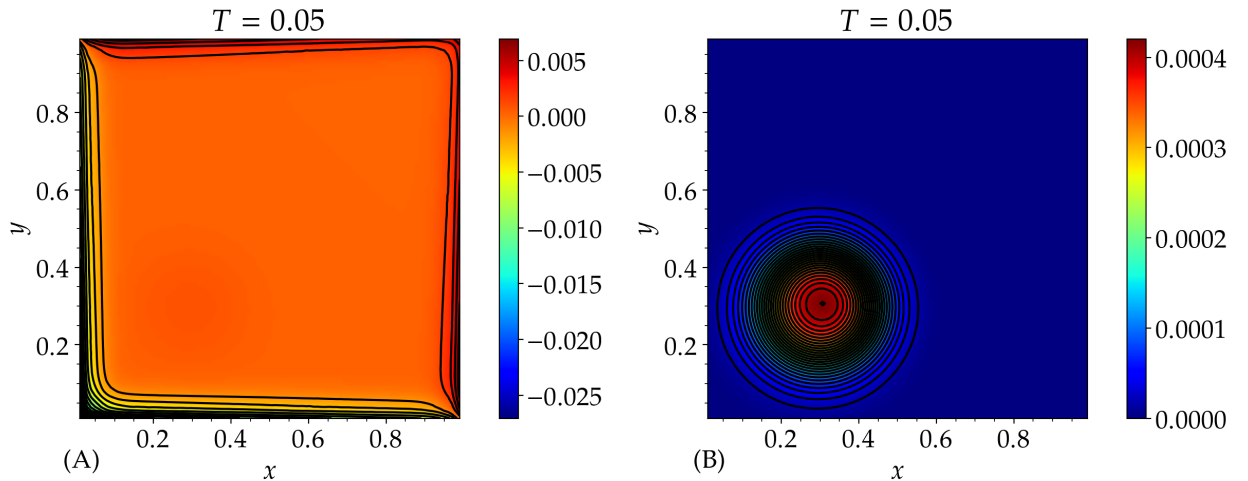


FIGURE 6. Pseudo-colour plots and contours of the density perturbations obtained by (A) the non well-balanced explicit scheme and (B) the well-balanced scheme at time $T = 0.05$ with $\varepsilon = 1$ and $\zeta = 10^{-3}$.

Next, we assess the performance of the schemes in the stiff regimes by setting $\varepsilon = 0.1$ and 0.01 . In order to keep the data well-prepared, we set $\zeta = \varepsilon^2$ as before. Similar to the 1D case, the non well-balanced code crashes for the chosen values of ε . Figure 7 clearly indicates that well-balanced AP scheme is able to accurately resolve the circular structure of the perturbations.

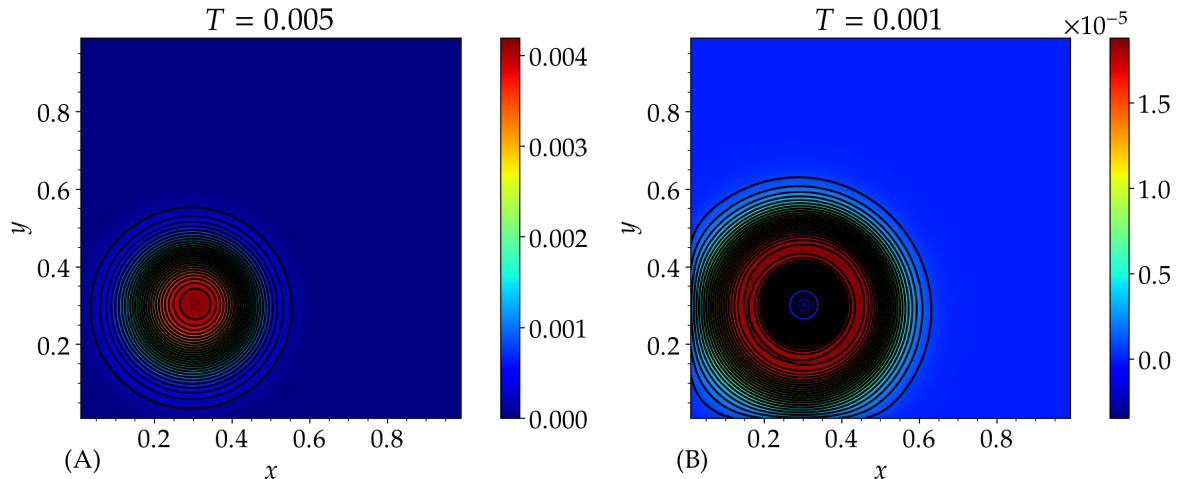


FIGURE 7. Pseudo-colour plots and contours of the density perturbation computed using the well-balanced scheme. (A) $\varepsilon = 0.1$, $T = 0.005$ (B) $\varepsilon = 0.01$, $T = 0.001$.

8.6. Stationary Vortex. We consider the following test problem inspired by [43] which simulates a stationary vortex under the action of a gravitational field. The vortex test problem is a benchmark to assess the low Mach number properties of numerical schemes and the dependence of their dissipation on the Mach number. Since an exact stationary solution is available, we also make use this problem to corroborate the uniform first order convergence of the scheme with respect to ε .

The computational domain is $[0, 1] \times [0, 1]$, the pressure law is $\wp(\rho) = \rho^2$, and the gravitational potential is radially symmetric with $\phi(r) = r^2$, where $r = \sqrt{(x - 0.5)^2 + (y - 0.5)^2}$ denotes the distance from the center of the domain $(0.5, 0.5)$.

We define a radially symmetric and piecewise continuous angular velocity, independent of ϕ , as

$$u_\theta(r) = \begin{cases} a_1 r, & \text{if } r \leq r_1, \\ a_2 + a_3 r, & \text{if } r_1 < r \leq r_2, \\ 0, & \text{otherwise.} \end{cases}$$

Here the inner and outer radii are $r_1 = 0.2$, $r_2 = 0.4$ and the constants are chosen as

$$a_1 = \frac{\bar{a}}{r_1}, \quad a_2 = -\frac{\bar{a}r_2}{r_1 - r_2}, \quad a_3 = \frac{\bar{a}}{r_1 - r_2},$$

with $\bar{a} = 0.1$. Since the vortex is stationary and has zero radial velocity, it satisfies the balance

$$(8.7) \quad \frac{1}{\varepsilon^2} \partial_r \wp(\rho) = \frac{\rho u_\theta^2}{r} - \frac{1}{\varepsilon^2} \rho \partial_r \phi.$$

We choose $\rho(0) = 1$, use the given expressions for u_θ and ϕ , and integrate (8.7) to obtain the following stationary solution of the Euler system (2.1)-(2.2) in polar co-ordinates:

$$\begin{aligned}\rho(0, x, y) &= 1 + \frac{\varepsilon^2}{2} \int_0^r \frac{u_\theta^2(s)}{s} ds - \frac{1}{2} r^2, \\ u(0, x, y) &= u_\theta(r)(y - 0.5)/r, \\ v(0, x, y) &= u_\theta(r)(0.5 - x)/r.\end{aligned}$$

The computational domain is discretised into 25×25 , 50×50 , 100×100 , 200×200 and 400×400 mesh points and the final time is set to $T = 1$. Periodic boundary conditions are implemented on all sides of the domain.

The L^1 -errors in ρ , ρu and ρv about the stationary solution along with the experimental order of convergence (EOC) for different values of ε are tabulated in Table 2. The EOC values clearly indicate the uniform first order convergence of the scheme irrespective of the value of ε .

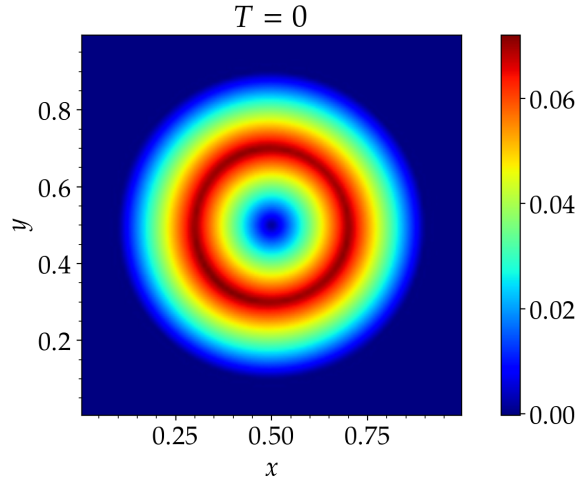
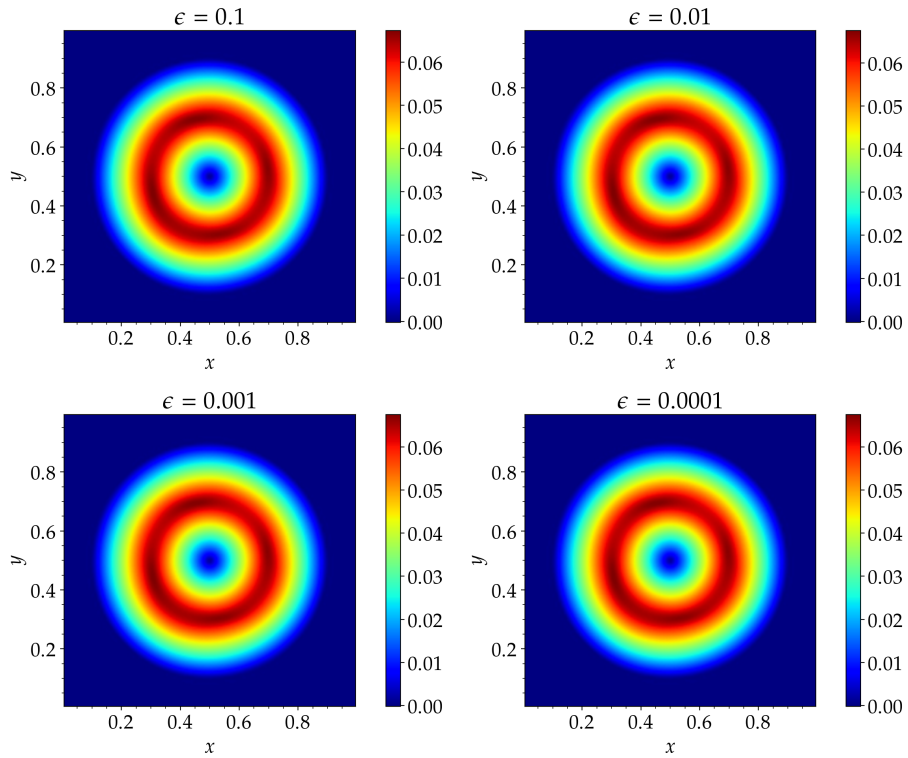
ε	$N_x = N_y$	L^1 -error in ρ	EOC	L^1 -error in ρu	EOC	L^1 -error in ρv	EOC
10^{-1}	25	8.3926E-07	–	1.2063E-03	–	1.2063E-03	–
	50	4.6492E-07	0.8521	6.4911E-04	0.8940	6.4911E-04	0.8940
	100	2.5632E-07	0.8590	3.5668E-04	0.8638	3.5668E-04	0.8638
	200	1.3345E-07	0.9416	1.8573E-04	0.9414	1.8573E-04	0.9414
	400	6.8504E-08	0.9620	9.4904E-05	0.9687	9.4904E-05	0.9687
10^{-2}	25	8.3044E-09	–	1.1826E-03	–	1.1826E-03	–
	50	4.4802E-09	0.8903	6.1962E-04	0.9325	6.1962E-04	0.9325
	100	2.3266E-09	0.9453	3.2613E-04	0.9259	3.2613E-04	0.9259
	200	1.2075E-09	0.9462	1.6965E-04	0.9429	1.6965E-04	0.9429
	400	6.3285E-10	0.9321	8.8317E-05	0.9418	8.8317E-05	0.9418
10^{-3}	25	8.2967E-11	–	1.1816E-03	–	1.1816E-03	–
	50	4.4623E-11	0.8948	6.1780E-04	0.9355	6.1780E-04	0.9355
	100	2.3021E-11	0.9548	3.2427E-04	0.9302	3.2427E-04	0.9302
	200	1.1800E-11	0.9642	1.6771E-04	0.9512	1.6771E-04	0.9512
	400	6.0366E-12	0.9670	8.5966E-05	0.9641	8.5966E-05	0.9641

TABLE 2. L^1 -errors and EOC with respect to the exact solution.

In order to assess the dissipation of the scheme and its dependence on ε , we compute the flow Mach numbers $M = \sqrt{(u^2 + v^2)/(\gamma p/\rho)}$, the relative kinetic energies and vorticities for different values of $\varepsilon \in \{10^{-1}, 10^{-2}, 10^{-3}, 10^{-4}\}$. A comparison of the initial Mach number with the ones at $T = 1$ for different values of ε in Figure 9 shows that the dissipation of the scheme is independent of ε as the distortion of the vortex remains the same for different ε . In order to further corroborate the above fact, we plot in Figure 10 the relative kinetic energies versus time and a cross-section of the vorticity at the final time. Clearly, the figures corresponding to different ε are indistinguishable.

9. CONCLUSIONS

We have constructed an energy stable, structure preserving, well-balanced and AP scheme for the barotropic Euler system with gravity in the anelastic limit. The energy stability is achieved by introducing a velocity shift in the convective fluxes of mass and momenta. The semi-implicit in time and finite volume in space scheme preserves the positivity of density and is weakly consistent with the continuous model upon mesh refinement. The numerical scheme admits the discrete hydrostatic states as solutions and the stability of numerical solutions with respect to relative energy leads to

FIGURE 8. Pseudo-colour plot of the flow Mach number at time $T = 0$.FIGURE 9. Pseudo-colour plots of the flow Mach number at time $T = 1$ for different values of ε .

the well-balancing feature. The AP property of the scheme is rigorously shown on the basis of a priori energy estimates.

Results from several benchmark case studies confirm the theoretical findings. Simulation of stationary initial data clearly shows that the scheme approximates hydrostatic steady states upto

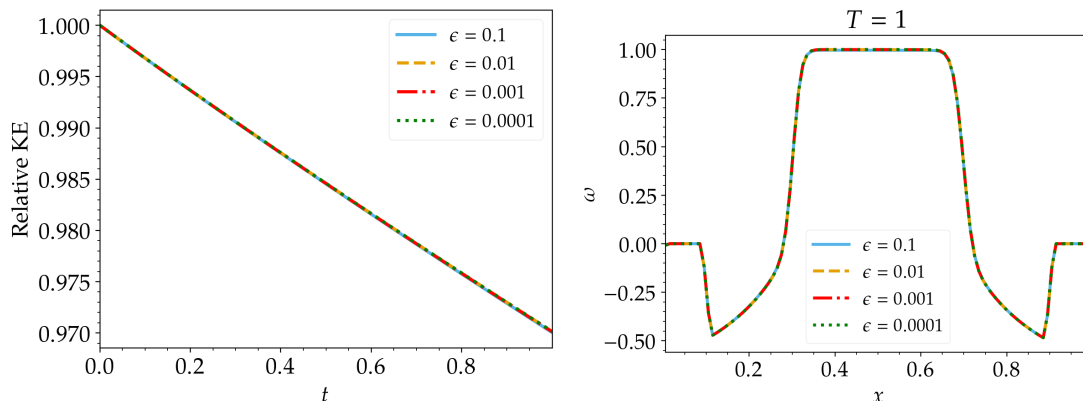


FIGURE 10. Comparison of relative kinetic energies (left) and cross sections of the vorticities (right) for different values of ε .

machine precision irrespective of the value of ε , which substantiate its well-balancing property. The proposed method can accurately resolve flows that arise from small perturbation of steady states, where a classical explicit scheme often fails. We have demonstrated the scheme's capabilities to maintain the positivity of density and to capture shock discontinuities in the compressible regime. The scheme performs well for a vortex benchmark for low Mach number flows and its dissipation seems uniform across different values of ε tending towards zero.

REFERENCES

- [1] K. R. Arun, R. Ghorai, and M. Kar. An asymptotic preserving and energy stable scheme for the barotropic Euler system in the incompressible limit. *J. Sci. Comput.*, 97(3):Paper No. 73, 31, 2023.
- [2] K. R. Arun, R. Ghorai, and M. Kar. An asymptotic preserving and energy stable scheme for the Euler-Poisson system in the quasineutral limit. *Appl. Numer. Math.*, 198:375–400, 2024.
- [3] E. Audusse, F. Bouchut, M.-O. Bristeau, R. Klein, and B. Perthame. A fast and stable well-balanced scheme with hydrostatic reconstruction for shallow water flows. *SIAM J. Sci. Comput.*, 25(6):2050–2065, 2004.
- [4] P. R. Bannon. On the anelastic approximation for a compressible atmosphere. *J. Atmospheric Sci.*, 53(23):3618–3628, 1996.
- [5] C. Birke, W. Boscheri, and C. Klingenberg. A well-balanced semi-implicit IMEX finite volume scheme for ideal magnetohydrodynamics at all Mach numbers. *J. Sci. Comput.*, 98(2):Paper No. 34, 26, 2024.
- [6] G. Bispen, K. R. Arun, M. Lukáčová-Medvid'ová, and S. Noelle. IMEX large time step finite volume methods for low Froude number shallow water flows. *Commun. Comput. Phys.*, 16(2):307–347, 2014.
- [7] S. Boscarino, F. Filbet, and G. Russo. High order semi-implicit schemes for time dependent partial differential equations. *J. Sci. Comput.*, 68(3):975–1001, 2016.
- [8] D. Bresch, M. Gisclon, and C.-K. Lin. An example of low Mach (Froude) number effects for compressible flows with nonconstant density (height) limit. *M2AN Math. Model. Numer. Anal.*, 39(3):477–486, 2005.
- [9] G. Bruell and E. Feireisl. On a singular limit for stratified compressible fluids. *Nonlinear Anal. Real World Appl.*, 44:334–346, 2018.
- [10] J. Březina and E. Feireisl. Measure-valued solutions to the complete Euler system. *J. Math. Soc. Japan*, 70(4):1227–1245, 2018.
- [11] N. Chaudhuri. Multiple scales and singular limits of perfect fluids. *J. Evol. Equ.*, 22(1):Paper No. 5, 32, 2022.
- [12] A. J. Chorin. Numerical solution of the Navier-Stokes equations. *Math. Comp.*, 22:745–762, 1968.
- [13] F. Couderc, A. Duran, and J.-P. Vila. An explicit asymptotic preserving low Froude scheme for the multilayer shallow water model with density stratification. *J. Comput. Phys.*, 343:235–270, 2017.
- [14] K. Deimling. *Nonlinear functional analysis*. Springer-Verlag, Berlin, 1985.
- [15] A. Duran, J.-P. Vila, and R. Baraille. Semi-implicit staggered mesh scheme for the multi-layer shallow water system. *C. R. Math. Acad. Sci. Paris*, 355(12):1298–1306, 2017.

- [16] A. Duran, J.-P. Vila, and R. Baraille. Energy-stable staggered schemes for the Shallow Water equations. *J. Comput. Phys.*, 401:109051, 24, 2020.
- [17] D. R. Durran. Improving the anelastic approximation. *J. Atmospheric Sci.*, 46(11):1453–1461, 1988.
- [18] D. R. Durran. *Numerical methods for wave equations in geophysical fluid dynamics*, volume 32 of *Texts in Applied Mathematics*. Springer-Verlag, New York, 1999.
- [19] R. Eymard, T. Gallouët, and R. Herbin. Finite volume methods. In *Handbook of numerical analysis, Vol. VII*, volume VII of *Handb. Numer. Anal.*, pages 713–1020. North-Holland, Amsterdam, 2000.
- [20] F. Fanelli and E. Zatorska. Low Mach number limit for the degenerate Navier-Stokes equations in presence of strong stratification. *Comm. Math. Phys.*, 400(3):1463–1506, 2023.
- [21] E. Feireisl, C. Klingenberg, O. Kreml, and S. Markfelder. On oscillatory solutions to the complete Euler system. *J. Differential Equations*, 269(2):1521–1543, 2020.
- [22] E. Feireisl and M. Lukáčová-Medvid'ová. Convergence of a mixed finite element–finite volume scheme for the isentropic Navier-Stokes system via dissipative measure-valued solutions. *Found. Comput. Math.*, 18(3):703–730, 2018.
- [23] E. Feireisl, J. Málek, A. Novotný, and I. Straškraba. Anelastic approximation as a singular limit of the compressible Navier-Stokes system. *Comm. Partial Differential Equations*, 33(1-3):157–176, 2008.
- [24] E. Feireisl and A. Novotný. *Singular limits in thermodynamics of viscous fluids*. Advances in Mathematical Fluid Mechanics. Birkhäuser Verlag, Basel, 2009.
- [25] U. S. Fjordholm, S. Mishra, and E. Tadmor. Well-balanced and energy stable schemes for the shallow water equations with discontinuous topography. *J. Comput. Phys.*, 230(14):5587–5609, 2011.
- [26] T. Gallouët, R. Herbin, and J.-C. Latché. On the weak consistency of finite volumes schemes for conservation laws on general meshes. *SeMA J.*, 76(4):581–594, 2019.
- [27] T. Gallouët, R. Herbin, and J.-C. Latché. Lax–Wendroff consistency of finite volume schemes for systems of non linear conservation laws: extension to staggered schemes. *SeMA J.*, 79(2):333–354, 2022.
- [28] T. Gallouët, R. Herbin, J.-C. Latché, and K. Mallem. Convergence of the marker-and-cell scheme for the incompressible Navier-Stokes equations on non-uniform grids. *Found. Comput. Math.*, 18(1):249–289, 2018.
- [29] T. Gallouët, R. Herbin, J.-C. Latché, and N. Therme. Consistent internal energy based schemes for the compressible Euler equations. 24:119–154, [2021] ©2021.
- [30] T. Gallouët, R. Herbin, D. Maltese, and A. Novotny. Error estimates for a numerical approximation to the compressible barotropic Navier-Stokes equations. *IMA J. Numer. Anal.*, 36(2):543–592, 2016.
- [31] L. Gosse. A well-balanced flux-vector splitting scheme designed for hyperbolic systems of conservation laws with source terms. *Comput. Math. Appl.*, 39(9-10):135–159, 2000.
- [32] R. Herbin, J.-C. Latché, Y. Nasserri, and N. Therme. A consistent quasi-second-order staggered scheme for the two-dimensional shallow water equations. *IMA J. Numer. Anal.*, 43(1):99–143, 2023.
- [33] R. Herbin, J.-C. Latché, and K. Saleh. Low Mach number limit of some staggered schemes for compressible barotropic flows. *Math. Comp.*, 90(329):1039–1087, 2021.
- [34] S. Jin. Asymptotic preserving (AP) schemes for multiscale kinetic and hyperbolic equations: a review. *Riv. Math. Univ. Parma (N.S.)*, 3(2):177–216, 2012.
- [35] R. Klein. Asymptotic analyses for atmospheric flows and the construction of asymptotically adaptive numerical methods. *ZAMM Z. Angew. Math. Mech.*, 80(11-12):765–777, 2000. Special issue on the occasion of the 125th anniversary of the birth of Ludwig Prandtl.
- [36] R. Klein. Asymptotics, structure, and integration of sound-proof atmospheric flow equations. *Theor. Comput. Fluid Dyn.*, 23(3):161–195, 2009.
- [37] D. Maltese and A. Novotný. Implicit MAC scheme for compressible Navier-Stokes equations: low Mach asymptotic error estimates. *IMA J. Numer. Anal.*, 41(1):122–163, 2021.
- [38] N. Masmoudi. Rigorous derivation of the anelastic approximation. *J. Math. Pures Appl. (9)*, 88(3):230–240, 2007.
- [39] M. S. Miesch, J. R. Elliott, J. Toomre, T. L. Clune, G. A. Glatzmaier, and P. A. Gilman. Three-dimensional spherical simulations of solar convection. I. Differential rotation and pattern evolution achieved with laminar and turbulent states. *The Astrophysical Journal*, 532(1):593, March 2000.
- [40] Y. Ogura and N. A. Phillips. Scale analysis of deep and shallow convection in the atmosphere. *J. Atmospheric Sci.*, 19(2):173–179, 1962.
- [41] A. Thomann, G. Puppo, and C. Klingenberg. An all speed second order well-balanced IMEX relaxation scheme for the Euler equations with gravity. *J. Comput. Phys.*, 420:109723, 25, 2020.
- [42] K. Xu. A well-balanced gas-kinetic scheme for the shallow-water equations with source terms. *J. Comput. Phys.*, 178(2):533–562, 2002.
- [43] M. Zenk. *On Numerical Methods for Astrophysical Applications*. Doctoral thesis, Universität Würzburg, 2018.

SCHOOL OF MATHEMATICS, INDIAN INSTITUTE OF SCIENCE EDUCATION AND RESEARCH THIRUVANANTHAPURAM,
THIRUVANANTHAPURAM 695551, INDIA
Email address: `arun@iisertvm.ac.in`, `mainak17@iisertvm.ac.in`